

# REVISITING LARS FOR LARGE BATCH TRAINING GENERALIZATION OF NEURAL NETWORKS

**Khoi Do<sup>◇♡</sup>, Duong Nguyen<sup>◇♣</sup>, Hoa Nguyen<sup>♡</sup>, Long Tran-Thanh<sup>★</sup>, and Quoc-Viet Pham<sup>♣</sup>**

<sup>♡</sup> Hanoi University of Science and Technology, <sup>★</sup> University of Warwick

<sup>♣</sup> Pusan National University, <sup>♠</sup> Trinity College Dublin, <sup>◇</sup> equal contribution

{khoido8899, mduongbkhn}@gmail.com, hoa.nguyentien@hust.edu.vn,

long.tran-thanh@warwick.ac.uk, viet.pham@tcd.ie

## ABSTRACT

LARS and LAMB have emerged as prominent techniques in Large Batch Learning (LBL), ensuring the stability of AI training. One of the primary challenges in LBL is convergence stability, where the AI agent usually gets trapped into the sharp minimizer. Addressing this challenge, a relatively recent technique, known as warm-up, has been employed. However, warm-up lacks a strong theoretical foundation, leaving the door open for further exploration of more efficacious algorithms. In light of this situation, we conduct empirical experiments to analyze the behaviors of the two most popular optimizers in the LARS family: LARS and LAMB, with and without a warm-up strategy. Our analyses give us a comprehension of the novel LARS, LAMB, and the necessity of a warm-up technique in LBL. Building upon these insights, we propose a novel algorithm called Time Varying LARS (TVLARS), which facilitates robust training in the initial phase without the need for warm-up. Experimental evaluation demonstrates that TVLARS achieves competitive results with LARS and LAMB when warm-up is utilized while surpassing their performance without the warm-up technique.

## 1 INTRODUCTION

Large Batch Learning (LBL) has become increasingly vital in modern deep learning (DL) due to its numerous advantages. Firstly, it improves efficiency by leveraging parallel processing, enabling faster model updates and reducing training time. Secondly, LBL enhances optimization stability by mitigating noisy gradients, resulting in smoother convergence and fewer gradient fluctuations during training. Thirdly, it improves generalization by exposing the model to a diverse range of samples, capturing underlying patterns, and improving overall performance. Moreover, LBL contributes to memory efficiency by reusing intermediate results and optimizing memory requirements. Finally, it enables better hardware utilization by effectively leveraging the parallel processing capabilities of modern hardware accelerators. These advantages make LBL particularly suitable for training large deep neural network (DNN) models and self-supervised learning (SSL) tasks, where increased model capacity and representation learning are crucial. Nonetheless, the present application of LBL with conventional gradient-based methods often necessitates the use of heuristic tactics and results in compromised generalization accuracy Hoffer et al. (2017); Keskar et al. (2017).

Numerous methods Huo et al. (2021); You et al. (2020); Fong et al. (2020) have been explored to address the performance issues associated with large-batch training. Among these methods, Layer-Wise Adaptive Rate Scaling (LARS) You et al. (2017) has gained significant popularity. Fundamentally, LARS employs adaptive rate scaling to improve gradient descent on a per-layer basis. As a result, training stability is enhanced across the layers of the DNN model. However, LARS exhibits a primary limitation: its performance tends to be unstable during the initial stages of the LBL process. This occurrence results in sluggish convergence during the early phase of learning, particularly when dealing with large batches. As an effective strategy to enhance the adaptive ratio scaling technique exists, warm-up reduces the LARS adaptive rate and thus results in a more stable learning process for larger batch sizes. However, it is worth noting that this approach relies on a somewhat indistinct tuning process and lacks a solid theoretical foundation. This gap offers ample opportunities for further exploration and improvement within the realm of adaptive rate scaling algorithms.

Through empirical experiments, we made an interesting observation in the initial phase of LARS training. The rate scaler value was found to be high due to the division between two norms ( $\|w\|/\|\nabla\mathcal{L}\|$ ), which was caused by the nearly 0 value of the layer-wise gradient  $\|\nabla w\|$ . This infinitesimal value of the layer-wise gradient was a consequence of getting trapped into sharp minimizers during the initial phase, leading to an explosion of the adaptively scaled gradient. To address this phenomenon, we propose a new algorithm called Time-Varying LARS (TVLARS), which enables gradient exploration for LARS in the initial phase while retaining the stability of other LARS family members in the latter phase. Instead of using warm-up, which linearly increases the gradient scale ratio at the beginning to stimulate searching over the initial sharp minimizers (which incurs redundant searching efforts), we begin the search from the high scaling ratio where searching is more efficient, aligning with theories about sharp minimizers in LBL Keskar et al. (2017). Our contributions can be summarized as follows:

- We performed empirical experiments on two seminal LBL techniques, namely LARS and LAMB, to gain a comprehensive understanding of how they enhance LBL performance.
- We investigated the necessity of warm-up for the LARS method and identified potential issues with using warm-up in LARS. These potential shortcomings arise from the lack of understanding regarding sharp minimizers aspects in LBL.
- Acknowledging the principles of LARS and the warm-up technique, we propose a simple and straightforward alternative technique, so-called TVLARS, which is more aligned with the theories about sharp minimizers in LBL.
- To validate the efficacy of TVLARS, we conduct several experimental evaluations, comparing its performance against other popular baselines. The results of our experiments demonstrate that TVLARS significantly outperforms the state-of-the-art benchmarks, particularly when the batch size becomes large (e.g., 8192, 16384).

## 2 NOTATIONS AND PRELIMINARIES

**Notation.** We denote by  $w_t \in \mathbb{R}^d$  the model parameters at time step  $t$ . For any function  $f : \mathbb{R}^d \rightarrow \mathbb{R}^d$ ,  $\nabla l(x_i, y_i|w^k)$  is denoted the gradient with respect to  $w^{(k)}$ . We use  $\|\cdot\|$  and  $\|\cdot\|_1$  to denote  $l_2$ -norm and  $l_1$ -norm of a vector, respectively. We start our discussion by formally stating the problem setup. In this paper, we study a non-convex stochastic optimization problem of the form:

$$\min_{w \in \mathbb{R}^d} \mathcal{L}(w) \triangleq \mathbb{E}_{x_i, y_i \sim P(X, Y)} [\ell(x_i, y_i|w)] + \frac{\lambda}{2} \|w\|^2, \quad (1)$$

where  $\ell$  is an empirical loss function,  $(x, y) \sim P(X, Y) \in Z = \{X, Y\}$  is sample and ground truth.

**LARS.** To deal with LBL, You et al. (2017) proposed LARS. Suppose a neural network has  $K$  layers, we have  $w = \{w^1, w^2, \dots, w^K\}$ . The learning rate at layer  $k$  is updated as follows:

$$\gamma_t^k = \gamma_{\text{scale}} \times \eta \times \frac{\|w_t^k\|_2}{\|\frac{1}{B} \sum_{i \in I_t} \nabla l(x_i, y_i|w_t^k)\|_2}, \quad (2)$$

where  $\gamma_{\text{scale}} = \gamma_{\text{target}} \times \frac{B}{B_{\text{base}}}$  in You et al. (2017) and  $\eta$  is the LARS coefficient for the LBL algorithm. Despite its practical effectiveness, there has inadequate theoretical insight into LARS. Additionally, without implementing warm-up techniques Goyal et al. (2018), LARS tends to exhibit slow convergence or divergence during initial training.

## 3 THE MYSTERY OF GENERALIZATION BEHIND WARM-UP LARS AND NON WARM-UP LARS

This section explores how the LARS optimizers contribute to large-batch training. By revealing the mechanism of large-batch training, we provide some insights for improving LARS performance. To understand the detrimental impact of lacking warm-up procedure in current state-of-the-art LBL techniques, we employ the LARS and LAMB optimizers on vanilla classification problems to observe the convergence behavior. We conduct empirical experiments on CIFAR10 Krizhevsky (2009).

**Algorithm 1** TVLARS algorithm

**Require:**  $w_t^k \in \mathbb{R}^d$ , learning rate  $\{\gamma_t^k\}_t^T$ , delay factor  $\lambda$ , batch size  $\mathcal{B}$ , delay epoch  $d_e$ , scaling factor  $\alpha$ , time-varying factor  $\phi_t$ , momentum  $\mu$ ,  $\eta$ ,  $\gamma_{\min}$ ,  
**for**  $e = 1 : N$  **do**  
  Sample  $\mathcal{B}$  samples  $\mathbb{B}_t = \{(x_t^1, y_t^1), \dots, (x_t^b, y_t^b)\}$   
  Compute gradient

$$\nabla_w^t \mathcal{L}(w) = \frac{1}{|\mathbb{B}_t|} \sum_{i=1}^b \nabla \ell(x_t^i, y_t^i | w).$$

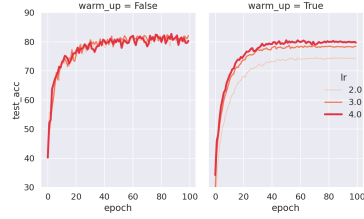
Update  $\phi_t = \frac{1}{\alpha + e^{\psi_t}} + \gamma_{\min}$  where  $\psi_t = \lambda(t - d_e)$   
  Compute layer learning rate

$$\gamma_t^k = \eta \times \phi_t \times \frac{\|w_t^k\|}{\|\nabla_w^t \mathcal{L}(w) + w_d\|}$$

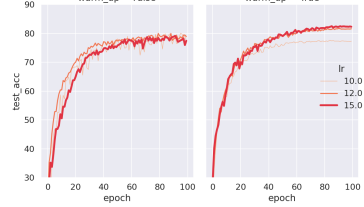
  Compute Momentum  $m_{t+1}^k = w_t^k - \gamma_t^k \nabla_w^t \mathcal{L}(w)$   
  Adjust model weight

$$w_{t+1}^k = m_{t+1}^k + \mu (m_{t+1}^k - m_t^k).$$

**end for**



(a) Test Accuracy -  $\mathcal{B} = 1024$



(b) Test Accuracy -  $\mathcal{B} = 8192$

Figure 1: LARS with and without warm-up analysis

### 3.1 ON THE PRINCIPLE OF LARS

First, we revisit the LARS algorithm, which proposes adaptive rate scaling. Essentially, LARS provides a learning rate (LR) that adapts prior to each neural network layer, as shown in Equation (2). From a geometric perspective on the neural network layer  $k$ , the norm of all weight components  $\|w_t^k\|$  can be seen as the length of the vector containing all components in the Euclidean vector space. Similarly, the norm of all gradient components  $\|\nabla \mathcal{L}(w_t^k)\|$  can be regarded as the length of the gradient vector of all components in the vector space. Thus, the scaling ratio  $\|w_t^k\|/\|\nabla \mathcal{L}(w_t^k)\|$  can be interpreted as the number of distinct pulses in Hartley’s law.

By considering this scaling ratio, we can adjust the layer-wise gradient based on the volume of the layer-wise weight parameters. In other words, instead of taking the normal gradient step  $\nabla w_t^k$  at every layer  $k$ , we perform a gradient step as a percentage of the total weight norm  $\|w^k\|$ . The proportional gradient update can be expressed as follows:

$$\eta \times \frac{\|w_t^k\|}{\|\nabla \mathcal{L}(w_t^k)\|} \times \nabla \mathcal{L}(w_t^{k,j}) = \eta \times \|w_t^k\| \times \frac{\nabla \mathcal{L}(w_t^{k,j})}{\|\nabla \mathcal{L}(w_t^k)\|}, \quad (3)$$

where  $\nabla \mathcal{L}(w_t^{k,j})$  is the gradient on  $j$ -th parameter in layer  $k$ .  $\frac{\nabla \mathcal{L}(w_t^{k,j})}{\|\nabla \mathcal{L}(w_t^k)\|}$  represents the gradient update percentage estimation function. It becomes apparent that the adaptive rate scaling function from LARS only influences the percentage update to the layer-wise model parameters. However, it does not address the issue of mitigating the problem of sharp minimizers in the initial phase of LBL.

### 3.2 LARS AND THE NECESSITY OF WARM-UP

The learning rate warm-up strategy is considered an important factor of LBL, which enhances the model performance and training stability You et al. (2020), Gotmare et al. (2019), Goyal et al. (2018), You et al. (2017). Starting with a small learning rate, the warm-up strategy linearly scales the learning rate to the target one, then switches to a regular learning rate decay, which is stated to reduce loss in accuracy, though its unproven empirical properties. Therefore, we conducted the analysis to investigate the vitality of warming up as well as its potential issues.

**Quantitative results.** Our quantification results on CIFAR10 are presented in Figure 1, showcasing the accuracy of training on the test dataset. From the figure, a notable disparity in AI performance is

observed when comparing runs with and without a warm-up strategy. In particular, the LARS without a warm-up technique, exhibits greater training instability, characterized by fluctuating accuracy. In addition, this performance deterioration becomes especially pronounced with larger batch sizes, resulting in a reduction of test accuracy by approximately 3 – 5% when LARS is employed without warm-up (further results can be found in Appendix F).

**From adaptive ratio to LBL performance.** To gain a deeper understanding of the adaptive rate scaling series, we conducted more comprehensive experiments accompanied by analyses of the adaptive ratio scaling values in LARS. Each experimental result in our research includes two key aspects: the test loss during the model’s training phase and the corresponding adaptive scaling ratio value (i.e.,  $\|w\|/\|\nabla\mathcal{L}(w)\|$ ). In our study, we examined the detailed results of LARS with the

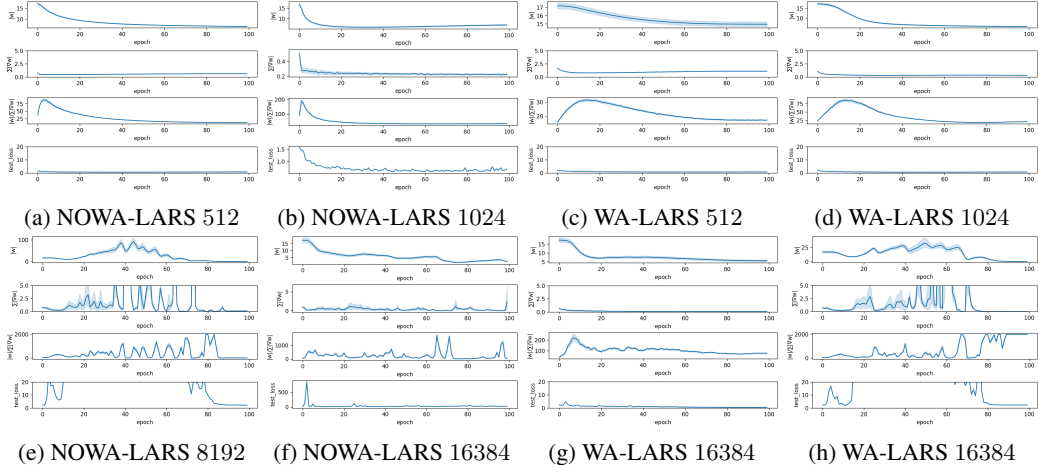


Figure 2: This figure illustrated the quantitative performance of LARS ( $B = 16K$ ) conducted with a warm-up (WA-LARS) and without a warm-up strategy (NOWA-LARS). Each figure contains 4 subfigures, which indicate the weight norm  $\|w\|$ , gradient norm  $\|\nabla w\|$ , and ratio  $\|w\|/\|\nabla w\|$  of all layers, and test loss value in the y axis.

warm-up strategy, as presented in Appendix E.2.1. We made observations regarding the convergence stability and the behavior of the scaling ratio in the model parameters’ norm, denoted as  $\|w_t^k\|$ :

- 1) During the initial phase of the successfully trained models (characterized by a significant reduction in test loss), the ratio  $\|(w_t^k)\|/\|\nabla\mathcal{L}(w_t^k)\|$  tends to be high, indicating a higher learning rate.
- 2) High variance in the scaling ratio indicates significant exploration during training, resulting in noticeable fluctuations in the model norm  $\|w\|$ . Conversely, when stability is required in training, the variance in the scaling ratio decreases accordingly.
- 3) Additionally, we noticed that it is necessary to impose an upper threshold on the scaling ratio to prevent divergence caused by values exceeding the range of  $\|\gamma_t^k \times \nabla\mathcal{L}\|$  over the model norm  $\|w\|$  You et al. (2017). The absence of the warm-up technique in LARS often leads to the scaling ratio surpassing this upper threshold. This issue is addressed by the warm-up aided LARS, where the scaling ratio during the initial phase is limited to values such as 0.15, 0.2, 0.3, 0.5, 1.5 (see Figures 18, 19, 20, 21, 22) compared to the warm-up LARS, where the highest scaling ratio is 0.06, 0.1, 0.125, 0.15, 0.25 (see Figures 12, 13, 14, 15, 16), respectively, with the highest learning rate at batch sizes of 512, 1024, 2048, 4096, 8192.
- 4) The scaling ratio in the warm-up-aided LARS is regulated by a more gradual incline. For example, after 40 – 50 epochs, the ratio decreases from 0.060 to 0.018 in Figure 12, 0.10 to 0.02, 0.125 to 0.027 in Figure 13, 0.16 to 0.048 in Figure 14, and 0.20 to 0.050 in Figure 15 for batch sizes of 512, 1024, 2048, 4096, respectively. On the other hand, in contrast to the warm-up assisted LARS, the vanilla LARS exhibits a steep decline in the scaling ratio. For instance, after 10 – 20 epochs, the ratio decreases from 0.15 to 0.048 in Figure 18, 0.221 to 0.032 in Figure 19, 0.30 to 0.043 in Figure 20, and 0.43 to 0.089 in Figure 21. For more comprehensive details and additional results, please refer to Appendix F.

**Extensive Study.** To gain deeper insights, we conducted additional experiments, and the results are presented in Figure 2. These figures contribute to a more thorough understanding of the empirical outcomes mentioned earlier in Section 3.2. Through the analysis of Section 3.2 and the insights derived from Figure 2, it becomes evident that the reduction in the adaptive ratio can be attributed to the rapid decrease in the magnitude of  $\|w_t^k\|$  over time. This phenomenon occurs in tandem with the exponential reduction of the denominator, which incorporates  $\|\nabla\mathcal{L}(w_t^k)\|$ . Consequently, we can deduce that the superior performance of the AI model with respect to larger batch sizes is a consequence of the gradual decrease in the norm of model parameters.

Put differently, envisioning the model parameters as a hypersphere, the gradient descent technique explores the topological space of this hypersphere. This exploration commences from the hypersphere’s edge, indicated by  $\|w_t^k\| = w_{\max}$ , and progresses toward its center, characterized by  $\|w_t^k\| = 0$ . This hypothesis finds support in the gradual decrease of  $\|w_t^k\|$  as depicted in Figure 2. Nevertheless, in cases of exploding gradient issues, significant fluctuations in  $\|w_t^k\|$  can disrupt the functionality of this hypothesis.

In the context of LARS without warm-up settings, the adaptive ratio experiences a steeper decline due to the rapid reduction in the parameter norm  $\|w_t^k\|$ . This heightened reduction rate can be understood as an overly swift exploration of the parameter vector hypersphere. Such expeditious exploration can result in overlooking numerous potential searches, leading to the potential failure to identify global minimizers. In contrast, with WA-LARS, the search across the parameter space occurs more gradually, ensuring a more stable exploration of the parameter hypersphere.

Based on the aforementioned observations, our conclusion is that the primary challenges encountered in the context of LARS stem from two key issues: a high layer-wise scaling ratio and substantial variance in the model norm, denoted as  $\|w\|$ . These dual challenges pose significant obstacles to LARS’s effective performance. As a solution, the warm-up process aims to prevent the occurrence of exploding gradients during the initial phase by initially setting the learning rate coefficient to a significantly low value and gradually increasing it thereafter. However, we believe that the application of the warm-up technique may be somewhat lacking in a comprehensive understanding. Consequently, we are motivated to delve deeper into the characteristics of sharp minimizers within the LBL, seeking a more profound insight into LARS and the warm-up process.

### 3.3 LARS AND THE POTENTIAL ISSUES OF WARM-UP

**The degradation in learning performance when the batch size becomes large and the sharp minimizer.** As mentioned in Section 3.1, the LARS technique only influences the percentage update to their layer-wise model parameters to stabilize the gradient update behavior. However, the learning efficiency is not affected by the LARS technique. To gain a better understanding of LARS performance as the batch size increases significantly, our primary goal is to establish an upper limit for the unbiased gradient, which is similar to (Wang et al., 2020, Assumption 2) (i.e., the variance of the batch gradient). We first adopt the following definition:

**Definition 1.** A gradient descent  $g_i^t$  at time  $t$  using reference data point  $x_i$  is a composition of a general gradient  $\bar{g}^t$  and a variance gradient  $\Delta g_i^t$ . For instance, we have  $g_i^t = \bar{g}^t + \Delta g_i^t$ , where the variance gradient  $\Delta g_i^t$  represents the perturbation of gradient descent over the dataset. The general gradient represents the invariant characteristics over all perturbations of the dataset.

The aforementioned definition leads to the following theorem that shows the relationship between unbiased gradient (Wang et al., 2020, Assumption 2) and the batch size as follows:

**Theorem 1** (Unbiased Large Batch Gradient). Given  $\bar{g}^t$  as mentioned in Definition 1,  $g_{\mathcal{B}}^t$  is the batch gradient with batch size  $\mathcal{B}$ . Given  $\sigma^2$  is the variance for point-wise unbiased gradient as mentioned in (Wang et al., 2020, Assumption 2), we have the stochastic gradient with  $\mathcal{B}$  is an unbiased estimator of the general gradient and has bounded variance:  $\mathbb{E}_{x_i, y_i \in \{\mathcal{X}, \mathcal{Y}\}} [g^t - g_{\mathcal{B}}^t] \leq \sigma^2 / \mathcal{B}$ ,

*Proof.* The proof is shown in Appendix B.

Theorem 1 demonstrates that utilizing a large batch size  $\mathcal{B}$  during training results in more stable gradients. However, two significant concerns have negative implications. Firstly, the stability of the gradient is influenced by the large batch. Consequently, in scenarios where the adaptive ratio experiences rapid reduction (as discussed in NOWA settings in Section 3.2), there is a potential for the gradient descent process to become trapped into sharp minimizers during the initial stages

Keskar et al. (2017). Secondly, due to the steep decline in the adaptive ratio, the exploration across the hypersphere of  $w_k^t$  occurs too swiftly (specifically, from  $w_{\max}$  to 0). Large batch (LB) techniques lack the exploratory characteristics of small batch (SB) methods and often focus excessively on narrowing down to the minimizer that is closest to the starting point Keskar et al. (2017).

**Potential issues of Warm-up in LARS.** Warm-up is a widely employed technique in LARS. It involves initially scaling the base learning rate and subsequently reducing it to facilitate gradient exploration. However, our findings indicate that gradually increasing the base learning rate from an extremely low value before gradient exploration is unnecessary. When the base learning rate is too small, particularly at the outset, learning fails to avoid memorizing noisy data You et al. (2019). Furthermore, when the model gets trapped in the sharp minimizers during the warm-up process, due to the steepness of the sharp minimizers, the model will be unable to escape from the sharp minima. Moreover, apart from the high variance of the gradient of mini-batch learning, the gradient of the LBL is stable as mentioned in theorem 1. Therefore, the LBL is halted until the learning rate surpasses a certain threshold.

## 4 METHODOLOGY

After conducting and comprehending the experiential quantification in Section 3, we have identified the issues of warm-up LARS. It becomes evident that the adaptive learning rate scaling is not well-aligned with the characteristics of sharp minimizer distributions in the context of large batch settings. Specifically, during the initial phases of the search process, the loss landscape tends to exhibit numerous sharp minimizers that necessitate sufficiently high gradients to facilitate efficient exploration. Furthermore, it is imperative for the learning rate to be adjustable so that the LBL can be fine-tuned to match the behavior of different datasets and learning models.

To this end, we propose a novel algorithm called Time-Varying Layer-wise Adaptive Rate Scaling (TVLARS) for large-batch deep learning optimization, that aims to take full advantage of the strength of LARS and warm-up strategy along with drawbacks avoidance. A key idea of TVLARS is to ensure the following characteristics:

**1) Initiating Exploration Stimulus.** Although warm-up strategy enhances model training stability (Section 3), learning from a strictly small learning rate prevents the model from tackling poor sharp minimizers, appearing much near initialization point Granzol et al. (2022), Keskar et al. (2017), Dinh et al. (2017). Otherwise, as a result of the steep decline in adaptive ratio, the exploration around the hypersphere of  $w_k^t$  is restricted (Theorem 1) and does not address the sharp minimizer concern (Section 3.1). Moreover, the use of warm-up does not fulfill the need for LBL training as the unnecessary linear scaling (Section 3.3). We then construct TVLARS as an optimizer that uses a high initial learning rate owing to its ability of local sharp minima evasion, which enhances the loss function’s landscape exploration.

$$\phi_t = \frac{1}{\alpha + e^{\psi_t}} + \gamma_{\min} \quad \text{where} \quad \psi_t = \lambda(t - d_e) \quad (4)$$

**2) Learning Rate Decay.** To avoid instability of training due to the high initial learning rate, we use a parameter  $d_e$  specifying the number of delayed epochs as inspired by the warm-up strategy. After  $d_e$  epochs, the gradient scaling ratio is then annealed by Equation 4, which is the time-varying component used to tackle. According to the mathematical discussion of the LARS principle (Section 3.1) and the aforementioned characteristic of LARS, LAMB with and without a warm-up strategy (Section 3.2, 3.3), the adaptive ratio  $\frac{\|w\|}{\|\nabla\mathcal{L}(w)\|}$  tends to be exploding as the model is stuck at local sharp minima, then  $\|\nabla\mathcal{L}(w)\|$  decay faster than  $\|w\|$ .

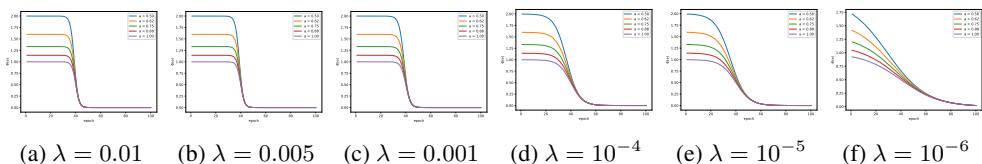


Figure 3: The decay plot of TVLARS algorithm under different settings.

**3) Configurable Decay Rate.** The proposed time-varying component  $\phi_t$  is constructed based on the sigmoid function whose curve is smooth to keep the model away from unstable learning (see Figure 3). Otherwise,  $\lambda$  is the soft-temperature factor, which controls the steepness of the time-variant component. Specifically, as  $\lambda$  is large, the steepness is significant, and the time-variant component  $\phi_t$  reduces faster. Therefore, by changing the soft-temperature factor  $\lambda$ , we can adjust the transition duration from gradient exploration to stable learning (i.e., we can achieve a stable learning phase faster as  $\lambda$  is larger, and otherwise).

**4) Alignment with LARS.** When the learning process is at the latter phase, the TVLARS behavior must be the same as LARS to inherit the LARS’s robustness (see Figure 3). We introduce two parameters  $\alpha$  and  $\gamma_{\min}$  used to control the bound for time-varying component  $\phi_t$ . For any  $\alpha, \gamma_{\min} \in \mathbb{R}$ , the lower and upper bounds for  $\phi_t$  is shown in Equation 5 (see proof in Appendix C).

$$\gamma_{\min} \leq \phi_t \leq \frac{1}{\alpha + \exp\{-\lambda d_e\}} \quad (5)$$

This boundary ensures that the gradient adaptive scaling ratio does not explode during the training phase. Otherwise, to guarantee that all experiments conducted are fair among optimizers,  $\alpha$  is set to 1, which means there is no increment in the initial learning rate after being chosen, and the minimum value of the learning rate is also set to  $\gamma_{\min}$ .

## 5 EXPERIMENT

Table 1: Accuracy (%) of LARS, LAMB, and TVLARS on a classification ( $\lambda = 10^{-4}$ ), and Barlow Twins problem ( $\lambda = 10^{-5}$ ). Bold numbers indicate better performance ( $\geq 1\%$  accuracy).

| Problem       | Classification |              |              |               |              |              | SSL - Barlow Twins |              |              |               |              |              |
|---------------|----------------|--------------|--------------|---------------|--------------|--------------|--------------------|--------------|--------------|---------------|--------------|--------------|
| Data set      | CIFAR10        |              |              | Tiny ImageNet |              |              | CIFAR10            |              |              | Tiny ImageNet |              |              |
| Learning rate | 1              | 2            | 3            | 1             | 2            | 3            | 1                  | 2            | 3            | 1             | 2            | 3            |
| LARS          | 74.64          | 77.49        | 79.64        | 33.72         | 36.60        | 38.92        | 51.31              | 58.89        | 60.76        | 18.32         | 19.52        | 21.12        |
| LAMB          | 57.88          | 64.76        | 78.39        | 20.28         | 41.40        | 37.52        | 10.01              | 12.01        | 67.31        | 13.46         | 17.75        | 27.37        |
| TVLARS        | <b>78.92</b>   | <b>81.42</b> | <b>81.56</b> | <b>37.56</b>  | <b>39.28</b> | <b>39.64</b> | <b>69.96</b>       | <b>69.72</b> | <b>70.54</b> | <b>29.02</b>  | <b>31.01</b> | <b>31.44</b> |
| Learning rate | 2              | 3            | 4            | 2             | 3            | 4            | 2                  | 3            | 4            | 2             | 3            | 4            |
| LARS          | 74.7           | 78.83        | 80.52        | 33.8          | 36.84        | 38.52        | 61.13              | 67.03        | 68.98        | 19.96         | 19.36        | 20.38        |
| LAMB          | 52.06          | 57.83        | 79.98        | 16.88         | 31.84        | 37.76        | 12.03              | 15.03        | 69.49        | 16.44         | 16.70        | 24.53        |
| TVLARS        | <b>81.84</b>   | <b>82.58</b> | <b>82.54</b> | <b>39.60</b>  | <b>39.16</b> | <b>39.40</b> | <b>67.38</b>       | <b>69.80</b> | <b>71.13</b> | <b>28.98</b>  | <b>27.46</b> | <b>28.32</b> |
| Learning rate | 5              | 6            | 7            | 5             | 6            | 7            | 5                  | 6            | 7            | 5             | 6            | 7            |
| LARS          | 75.22          | 79.49        | 81.1         | 34.48         | 38.04        | 40.44        | 52.42              | 57.35        | 52.42        | 19.92         | 20.33        | 19.98        |
| LAMB          | 43.12          | 47.88        | 81.43        | 12.60         | 18.56        | 39.92        | 10.01              | 15.64        | 60.08        | 18.67         | 21.98        | 23.43        |
| TVLARS        | <b>81.52</b>   | <b>82.22</b> | <b>82.44</b> | <b>39.56</b>  | <b>39.56</b> | <b>41.68</b> | <b>62.61</b>       | <b>61.71</b> | <b>61.05</b> | <b>26.15</b>  | <b>23.43</b> | <b>27.08</b> |
| Learning rate | 8              | 9            | 10           | 8             | 9            | 10           | 8                  | 9            | 10           | 8             | 9            | 10           |
| LARS          | 75.63          | 80.96        | 82.49        | 34.24         | 38.56        | 40.40        | 52.77              | 55.74        | 55.98        | 19.45         | 20.20        | 20.25        |
| LAMB          | 22.32          | 37.52        | 81.53        | 05.24         | 10.76        | 39.00        | 48.93              | 50.19        | 53.38        | 13.78         | 15.66        | 21.45        |
| TVLARS        | <b>80.9</b>    | <b>80.96</b> | <b>81.16</b> | <b>38.28</b>  | <b>39.96</b> | <b>41.64</b> | <b>57.96</b>       | <b>58.28</b> | <b>60.46</b> | <b>24.29</b>  | <b>24.29</b> | <b>24.92</b> |
| Learning rate | 10             | 12           | 15           | 10            | 12           | 15           | 10                 | 12           | 15           | 10            | 12           | 15           |
| LARS          | 77.59          | 81.75        | 82.5         | 34.36         | 38.12        | 42.00        | 50.29              | 52.78        | 09.65        | 19.69         | 20.79        | 21.62        |
| LAMB          | 16.14          | 19.85        | 81.78        | 01.12         | 02.48        | 39.20        | 42.22              | 45.26        | 52.39        | 19.60         | 23.44        | 23.55        |
| TVLARS        | <b>81.16</b>   | <b>82.42</b> | <b>82.74</b> | <b>36.48</b>  | <b>39.20</b> | 42.32        | <b>54.14</b>       | <b>53.56</b> | 52.24        | <b>23.41</b>  | <b>23.47</b> | <b>24.26</b> |
| Learning rate | 15             | 17           | 19           | 15            | 17           | 19           | 15                 | 17           | 19           | 15            | 17           | 19           |
| LARS          | 79.46          | 80.62        | 38.57        | 35.60         | 39.72        | 41.72        | 48.27              | 48.26        | 49.05        | 20.97         | 21.54        | 22.42        |
| LAMB          | 14.82          | 11.97        | 77.16        | 00.84         | 00.92        | 37.28        | 42.26              | 44.02        | 49.65        | 20.34         | 23.58        | 23.78        |
| TVLARS        | 79.20          | 80.42        | <b>80.42</b> | <b>38.56</b>  | <b>40.32</b> | 41.08        | 48.16              | <b>49.84</b> | <b>50.15</b> | <b>25.82</b>  | <b>24.95</b> | <b>25.91</b> |

### 5.1 CLASSIFICATION AND BARLOW TWINS PROBLEM

Table 1 demonstrates the performance achieved by the model trained with LARS, LAMB, and TVLARS, where the comprehensive experiment settings are stated in Appendix A. The table contains 2 main columns for CIFAR and Tiny ImageNet with associated tasks: CLF and BT (4 sub-columns except the first one). Besides CIFAR, Tiny ImageNet is considered to be a rigorously challenging dataset, which contains 100,000 images of 200 classes (500 for each class), hence it is suitable for evaluating the performance of LBL SSL tasks. Each experiment is implemented with one batch size and three related learning rates (detailedly stated at 5.2.2. Overall, TVLARS achieves

higher accuracy than LARS and LAMB for almost all settings considered. TVLARS tends to outperform LARS 4 ~ 7%, 3 ~ 4%, and 1 ~ 2% in each pair of  $\gamma_{\text{target}}$  and  $\mathcal{B}$ . LARS and LAMB, on the other hand, are immobilized by the poor sharp minima causing slow convergence. This is a result of the ratio  $\|w\|/\|\nabla_w \mathcal{L}(w)\| \rightarrow \infty$  as  $\|\nabla_w \mathcal{L}(w)\| \rightarrow 0$  (see Figure 2), which although creates a high adaptive learning rate to escape the trapped minima, the ratio  $\frac{\nabla_w \mathcal{L}(w)}{\|\nabla_w \mathcal{L}(w)\|}$  only influences the percentage update to the layer-wise model parameters hence cannot tackle the problem of sharp minima thoroughly (further analysis is available at 3, D, E). This phenomenon caused by the warm-up strategy partly indicates that LARS and LAMB are not only prevented from fast convergence but also stuck at poor sharp minima. While TVLARS ( $\lambda = 10^{-3}$ ) reach the optimum after 20 epochs, compared to 60 ~ 80 epochs from LARS and LAMB ( $\gamma_{\text{target}} = 19, \mathcal{B} = 16K$ ). See more associated results at D, E.1, E.2.

## 5.2 ABLATION TEST

### 5.2.1 DECAY COEFFICIENTS

Decay coefficient  $\lambda$  ( $\lambda \in \{0.01, 0.005, 0.001, 10^{-4}, 10^{-5}, 10^{-6}\}$ ) is a simple regularized parameter, which can be used to anneal the learning rate to enhance the model performance. Figure 4 demonstrate the quantitative result of experiments ( $\mathcal{B} \in \{1024, 16384\}$ ) conducted with different value of  $\lambda$  (see more results at D, E.3, G). Otherwise, to conduct a fair comparison between optimizers, we set the scaling factor  $\alpha = 1$ , so that the  $\gamma_{\text{target}}$  for all experiments are the same. The number of delayed epochs  $d_e$ , besides, is set to 10 epochs.

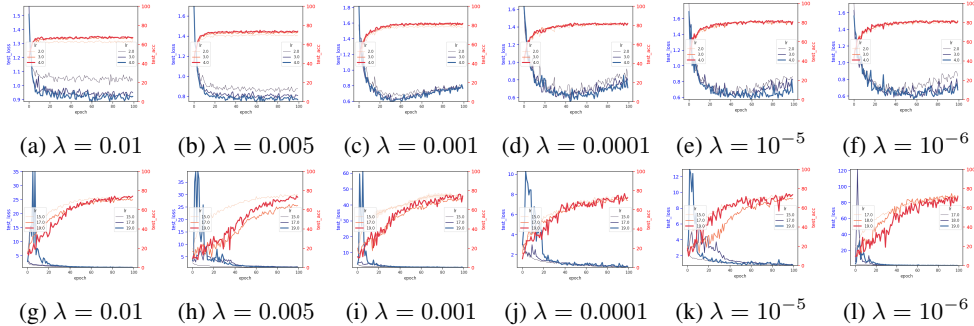


Figure 4: Quantitative comparison between stability in learning between experiments ( $\mathcal{B} \in \{1024, 16384\}$ , which are upper and lower row, respectively)

In 1K batch-sized experiments conducted with various  $\lambda$ , we observe that there is a large generalization gap among  $\gamma_{\text{target}}$  in  $\lambda \in \{0.01, 0.005\}$ , compared to the model performance achieved results in other  $\lambda$  values. Smaller  $\lambda$ , otherwise, enhance the model accuracy by leaving  $\gamma_{\text{target}}$  to stay nearly unchanged longer, which boosts the ability to explore loss landscape and avoid sharp minima. As a result, the model achieve higher accuracy: ~ 84% ( $\lambda = 10^{-5}$ ), compared to result stated in 1 ( $\lambda = 0.0001$ ). See D, G for detailed analysis and discussion. In contrast, the model performs better with larger values of  $\lambda$  ( $\lambda \in \{0.01, 0.005, 0.001\}$ ) in 16K batch-sized experiments. Owing to the pretty high initial  $\gamma_{\text{target}}$ , the model tends to find it easier to escape the local minima which do not converge within 20 epochs (4x compared to LARS) but also to a low loss value (~ 2), compared to just under 20 ( $\lambda = 10^{-6}$ ). This problem is owing to the elevated  $\gamma_{\text{target}}$ , which makes the leaning direction fluctuate dramatically in the latter training phase (see Figures 4j, 4k, 4l).

### 5.2.2 LEARNING RATE

A high initial learning rate, on the other hand, plays a pivotal role in enhancing the model performance by sharp minimizer avoidance Keskar et al. (2017); Dinh et al. (2017). Authors of Granzio et al. (2022); Krizhevsky (2014) suggest that, when multiplying the batch size by  $k$ , the learning rate should be  $\epsilon\sqrt{k}$  to keep the variance, where  $\epsilon$  is the learning rate used with  $\mathcal{B}_{\text{base}}$ . However, choosing  $\epsilon$  is an empirical way that there can be many applicable learning rates for any batch size  $\mathcal{B}$ . Therefore we not only apply the theorem from Keskar et al. (2017) but also conduct the experiments of each

batch size with many learning rates in a large variation to analyze how learning rate can affect the model performance. Figure 5 illustrates that the higher the learning rate is, the lower the loss value and the higher the accuracy model can achieve. According to Table 1, in the TVLARS experiment, the accuracy increases 1 ~ 3% and 2 ~ 6% in CLF and BT tasks, respectively (see detail analysis at D, E).

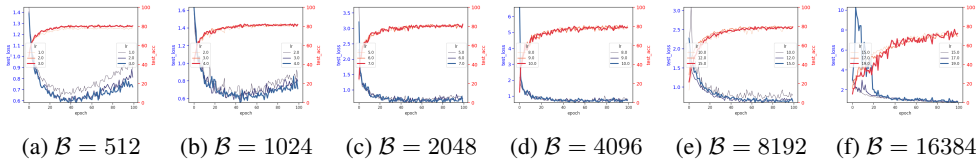


Figure 5: Quantitative analysis of the learning rates effect on correlated batch sizes ( $\lambda = 0.0001$ ).

## 6 RELATED WORKS

**Large-batch learning.** In Codreanu et al. (2017), several learning rate schedulers are proposed to figure out problems in LBL, especially the Polynomial Decay technique which helps ResNet50 converge within 28 minutes by decreasing the learning rate to its original value over several training iterations. Since schedulers are proven to be useful in LBL, You et al. (2017), Peng et al. (2018) suggested a learning rate scheduler based on the accumulative steps and a GPU cross Batch Normalization. Gotmare et al. (2019), besides, investigates deeper into the behavior of cosine annealing and warm-up strategy then shows that the latent knowledge shared by the teacher in knowledge distillation is primarily disbursed in the deeper layers. Inheriting the previous research, Goyal et al. (2018) proposed a hyperparameter-free linear scaling rule used for learning rate adjustment by constructing a relationship between learning rate and batch size as a function.

**Adaptive optimizer.** Another orientation is optimization improvement, starting by You et al. (2017), which proposed LARS optimizers that adaptively adjust the learning rate for each layer based on the local region. To improve LARS performance, Jia et al. (2018) proposed two training strategies including low-precision computation and mixed-precision training. In contrast, Liu & Mozafari (2022) authors propose JointSpar and JointSpar-LARS to reduce the computation and communication costs. On the other hand, Accelerated SGD Yamazaki et al. (2019), is proposed for training DNN in large-scale scenarios. In You et al. (2020), Xu et al. (2023), new optimizers called LAMB and SLAMB were proved to be successful in training Attention Mechanisms along with the convergence analysis of LAMB and LARS. With the same objective AGVM Xue et al. (2022) is proposed to boost RCNN training efficiency. Authors in Fong et al. (2020), otherwise proposed a variant of LAMB called LAMBC which employs trust ratio clipping to stabilize its magnitude and prevent extreme values. CLARS Huo et al. (2021), otherwise is suggested to exchange the traditional warm-up strategy owing to its unknown theory.

## 7 CONCLUSION

Given the current lack of clarity in fine-tuning and enhancing the performance of layerwise adaptive learning rates in LBL, we conducted experiments to gain deeper insights into layerwise-based update algorithms. We then devised an algorithm, referred to as TVLARS, based on our understanding of these algorithms and their interaction with LBL. Our TVLARS approach capitalizes on the observation that large batch learning often encounters sharper minimizers during the initial stages. By prioritizing gradient exploration, we facilitate more efficient navigation through these initial obstacles in large batch learning (LBL). Simultaneously, through adjustable discounts in layerwise learning rates, TVLARS combines the favorable aspects of a sequence of layerwise adaptive learning rates to ensure strong convergence in LBL. With our straightforward TVLARS algorithm, we achieve significantly improved convergence compared to two other cutting-edge methods, LARS and LAMB, particularly when dealing with extremely large batch sizes (e.g.,  $B = 16384$ ), across Tiny ImageNet and CIFAR-10 datasets.

## REFERENCES

- Martín Abadi, Paul Barham, Jianmin Chen, Zhifeng Chen, Andy Davis, Jeffrey Dean, Matthieu Devin, Sanjay Ghemawat, Geoffrey Irving, Michael Isard, Manjunath Kudlur, Josh Levenberg, Rajat Monga, Sherry Moore, Derek G. Murray, Benoit Steiner, Paul Tucker, Vijay Vasudevan, Pete Warden, Martin Wicke, Yuan Yu, and Xiaoqiang Zheng. Tensorflow: A system for large-scale machine learning. In *Proceedings of the 12th USENIX Conference on Operating Systems Design and Implementation, OSDI'16*, pp. 265–283, USA, Nov. 2016. USENIX Association.
- Adrien Bardes, Jean Ponce, and Yann LeCun. VICReg: Variance-invariance-covariance regularization for self-supervised learning. In *International Conference on Learning Representations*, 2022.
- Ting Chen, Simon Kornblith, Mohammad Norouzi, and Geoffrey Hinton. A simple framework for contrastive learning of visual representations. In *Proceedings of the International Conference on Machine Learning*, volume 119 of *Proceedings of Machine Learning Research*, pp. 1597–1607, 13–18 Jul 2020.
- Valeriu Codreanu, Damian Podareanu, and Vikram Saletore. Scale out for large minibatch sgd: Residual network training on imagenet-1k with improved accuracy and reduced time to train. *arXiv Preprint arXiv:1711.04291*, 2017.
- Jia Deng, Wei Dong, Richard Socher, Li-Jia Li, Kai Li, and Li Fei-Fei. Imagenet: A large-scale hierarchical image database. In *Proceedings of the IEEE/CVF Conference on Computer Vision and Pattern Recognition (CVPR)*, pp. 248–255. IEEE, 2009.
- Laurent Dinh, Razvan Pascanu, Samy Bengio, and Yoshua Bengio. Sharp minima can generalize for deep nets. In Doina Precup and Yee Whye Teh (eds.), *Proceedings of the International Conference on Machine Learning*, volume 70 of *Proceedings of Machine Learning Research*, pp. 1019–1028. PMLR, 06–11 Aug 2017.
- Rick Durrett. *Probability: Theory and Examples*. Cambridge Series in Statistical and Probabilistic Mathematics. Cambridge University Press, 4 edition, 2010. doi: 10.1017/CBO9780511779398.
- Jeffrey Fong, Siwei Chen, and Kaiqi Chen. Improving layer-wise adaptive rate methods using trust ratio clipping, 2020.
- Akhilesh Gotmare, Nitish Shirish Keskar, Caiming Xiong, and Richard Socher. A closer look at deep learning heuristics: Learning rate restarts, warmup and distillation. In *International Conference on Learning Representations*, May 2019.
- Priya Goyal, Piotr Dollár, Ross Girshick, Pieter Noordhuis, Lukasz Wesolowski, Aapo Kyrola, Andrew Tulloch, Yangqing Jia, and Kaiming He. Accurate, large minibatch sgd: Training imagenet in 1 hour, 2018.
- Diego Granzio, Stefan Zohren, and Stephen Roberts. Learning rates as a function of batch size: A random matrix theory approach to neural network training. *Journal of Machine Learning Research*, 23(173):1–65, 2022.
- Kaiming He, Xiangyu Zhang, Shaoqing Ren, and Jian Sun. Delving deep into rectifiers: Surpassing human-level performance on imagenet classification. In *Proceedings of the IEEE/CVF International Conference on Computer Vision (ICCV)*, pp. 1026–1034, 2015.
- Kaiming He, Xiangyu Zhang, Shaoqing Ren, and Jian Sun. Deep residual learning for image recognition. In *Proceedings of the IEEE/CVF Conference on Computer Vision and Pattern Recognition (CVPR)*, Jun. 2016.
- Elad Hoffer, Itay Hubara, and Daniel Soudry. Train longer, generalize better: closing the generalization gap in large batch training of neural networks. In I. Guyon, U. Von Luxburg, S. Bengio, H. Wallach, R. Fergus, S. Vishwanathan, and R. Garnett (eds.), *Advances in Neural Information Processing Systems*, Dec. 2017.
- Lei Huang, Dawei Yang, Bo Lang, and Jia Deng. Decorrelated batch normalization. In *Proceedings of the IEEE/CVF Conference on Computer Vision and Pattern Recognition (CVPR)*, June 2018.

- Zhouyuan Huo, Bin Gu, and Heng Huang. Large batch optimization for deep learning using new complete layer-wise adaptive rate scaling. *Proceedings of the AAAI Conference on Artificial Intelligence*, 35(9):7883–7890, May 2021.
- Xiyan Jia, Shutao Song, Wei He, Yangzihao Wang, Haidong Rong, Feihu Zhou, Liqiang Xie, Zhenyu Guo, Yuanzhou Yang, Liwei Yu, Tiegang Chen, Guangxiao Hu, Shaohuai Shi, and Xi-aowen Chu. Highly scalable deep learning training system with mixed-precision: Training imagenet in four minutes. *arXiv Preprint arXiv:1807.11205*, 2018.
- Yangqing Jia, Evan Shelhamer, Jeff Donahue, Sergey Karayev, Jonathan Long, Ross Girshick, Sergio Guadarrama, and Trevor Darrell. Caffe: Convolutional architecture for fast feature embedding. In *Proceedings of the 22nd ACM International Conference on Multimedia*, pp. 675–678, New York, NY, USA, Nov. 2014. Association for Computing Machinery.
- Nitish Shirish Keskar, Dheevatsa Mudigere, Jorge Nocedal, Mikhail Smelyanskiy, and Ping Tak Peter Tang. On large-batch training for deep learning: Generalization gap and sharp minima. In *International Conference on Learning Representations*, 2017.
- J. Kiefer and J. Wolfowitz. Stochastic Estimation of the Maximum of a Regression Function. *The Annals of Mathematical Statistics*, 23(3):462 – 466, 1952. doi: 10.1214/aoms/1177729392.
- Chiheon Kim, Saehoon Kim, Jongmin Kim, Donghoon Lee, and Sungwoong Kim. Automated learning rate scheduler for large-batch training. In *8th ICML Workshop on Automated Machine Learning (AutoML)*, 2021.
- Alex Krizhevsky. Learning multiple layers of features from tiny images. pp. 32–33, 2009.
- Alex Krizhevsky. One weird trick for parallelizing convolutional neural networks. *arXiv Preprint arXiv:1404.5997*, Oct. 2014.
- Yuanzhi Li, Colin Wei, and Tengyu Ma. Towards explaining the regularization effect of initial large learning rate in training neural networks. In *Advances in Neural Information Processing Systems*, Dec. 2019.
- Rui Liu and Barzan Mozafari. Communication-efficient distributed learning for large batch optimization. In Kamalika Chaudhuri, Stefanie Jegelka, Le Song, Csaba Szepesvari, Gang Niu, and Sivan Sabato (eds.), *Proceedings of the 39th International Conference on Machine Learning*, volume 162 of *Proceedings of Machine Learning Research*, pp. 13925–13946. PMLR, 17–23 Jul 2022.
- Ilya Loshchilov and Frank Hutter. SGDR: Stochastic gradient descent with warm restarts. In *International Conference on Learning Representations*, May 2017.
- Adam Paszke, Sam Gross, Francisco Massa, Adam Lerer, James Bradbury, Gregory Chanan, Trevor Killeen, Zeming Lin, Natalia Gimelshein, Luca Antiga, Alban Desmaison, Andreas Kopf, Edward Yang, Zachary DeVito, Martin Raison, Alykhan Tejani, Sasank Chilamkurthy, Benoit Steiner, Lu Fang, Junjie Bai, and Soumith Chintala. Pytorch: An imperative style, high-performance deep learning library. In *Advances in Neural Information Processing Systems*, volume 32, Dec. 2019.
- Chao Peng, Tete Xiao, Zeming Li, Yuning Jiang, Xiangyu Zhang, Kai Jia, Gang Yu, and Jian Sun. Megdet: A large mini-batch object detector. In *Proceedings of the IEEE/CVF Conference on Computer Vision and Pattern Recognition (CVPR)*, Jun. 2018.
- Jianyu Wang, Qinghua Liu, Hao Liang, Gauri Joshi, and H. Vincent Poor. Tackling the objective inconsistency problem in heterogeneous federated optimization. In *Advances in Neural Information Processing Systems*, volume 33, pp. 7611–7623, Dec. 2020.
- Hang Xu, Wenxuan Zhang, Jiawei Fei, Yuzhe Wu, Tingwen Xie, Jun Huang, Yuchen Xie, Mohamed Elhoseiny, and Panos Kalnis. SLAMB: Accelerated large batch training with sparse communication. In Andreas Krause, Emma Brunskill, Kyunghyun Cho, Barbara Engelhardt, Sivan Sabato, and Jonathan Scarlett (eds.), *Proceedings of the 40th International Conference on Machine Learning*, volume 202 of *Proceedings of Machine Learning Research*, pp. 38801–38825. PMLR, 23–29 Jul 2023.

- Zeyue Xue, Jianming Liang, Guanglu Song, Zhuofan Zong, Liang Chen, Yu Liu, and Ping Luo. Large-batch optimization for dense visual predictions. In Alice H. Oh, Alekh Agarwal, Danielle Belgrave, and Kyunghyun Cho (eds.), *Advances in Neural Information Processing Systems*, 2022. URL <https://openreview.net/forum?id=kImIiKGqDFA>.
- Masafumi Yamazaki, Akihiko Kasagi, Akihiro Tabuchi, Takumi Honda, Masahiro Miwa, Naoto Fukumoto, Tsuguchika Tabaru, Atsushi Ike, and Kohta Nakashima. Yet another accelerated sgd: Resnet-50 training on imagenet in 74.7 seconds. *arXiv Preprint arXiv:1903.12650*, 2019.
- Zhuliang Yao, Yue Cao, Shuxin Zheng, Gao Huang, and Stephen Lin. Cross-iteration batch normalization. In *Proceedings of the IEEE/CVF Conference on Computer Vision and Pattern Recognition (CVPR)*, pp. 12331–12340, June 2021.
- Kaichao You, Mingsheng Long, Jianmin Wang, and Michael I. Jordan. How does learning rate decay help modern neural networks? *arXiv Preprint arXiv:1908.01878*, 2019.
- Yang You, Igor Gitman, and Boris Ginsburg. Large batch training of convolutional networks, 2017.
- Yang You, Jing Li, Sashank Reddi, Jonathan Hseu, Sanjiv Kumar, Srinadh Bhojanapalli, Xiaodan Song, James Demmel, Kurt Keutzer, and Cho-Jui Hsieh. Large batch optimization for deep learning: Training bert in 76 minutes. In *International Conference on Learning Representations*, 2020.
- Jure Zbontar, Li Jing, Ishan Misra, Yann LeCun, and Stephane Deny. Barlow twins: Self-supervised learning via redundancy reduction. In *Proceedings of the International Conference on Machine Learning*, volume 139 of *Proceedings of Machine Learning Research*, pp. 12310–12320, 18–24 Jul. 2021.

## A EXPERIMENTAL SETTINGS

**Problems.** The vanilla classification (CLF) and Self Supervised Learning (SSL) are conducted and evaluated by the accuracy (%) metric. Regarding the success of SSL, we conduct the SOTA Barlow Twins<sup>1</sup> (BT) Zbontar et al. (2021) to compare the performance between LARS, LAMB You et al. (2020), and TVLARS (ours). To be more specific, the BT SSL problem consists of two stages: SSL and CLF stage, conducted with 1000 and 100 epochs, respectively. The dimension space used in the first stage of BT is 4096 stated to be the best performance setting in Zbontar et al. (2021), along with two sub Fully Connected 2048 nodes layers integrated before the latent space layer. We also conduct the CLF stage of BT with vanilla Stochastic Gradient Descent (SGD) Kiefer & Wolfowitz (1952) along with the Cosine Annealing Loshchilov & Hutter (2017) scheduler as implemented by BT authors. The main results of CLF and BT tasks are shown at 5.1. See more results of LAMB You et al. (2020), LARS You et al. (2017), and TVLARS at E.1, E.2, E.3, separately.

**Datasets and Models.** To validate the performance of the optimizers, we consider two different data sets with distinct contexts: CIFAR10 Krizhevsky (2009) ( $32 \times 32$ , 10 modalities) and Tiny ImageNet Deng et al. (2009) ( $64 \times 64$ , 200 modalities). Otherwise, the two SOTA model architectures ResNet18 and ResNet34 He et al. (2016) are trained separately from scratch on CIFAR10 and TinyImageNet. To make a fair comparison between optimizers, the model weight is initialized in Kaiming Uniform Distribution He et al. (2015).

**Optimizers and Warm-up Strategy.** Specifically, we explore the characteristics of LARS and LAMB by applying them with and without a warm-up strategy, aiming to understand the adaptive ratio  $|w|/|\nabla\mathcal{L}(w)|$  (see more results at E.2, F. LARS and LAMB official source codes are implemented inside NVcaffe Jia et al. (2014) and Tensorflow Abadi et al. (2016). the Pytorch version of LARS used in this research is verified and referenced from Lightning Flash<sup>2</sup>. LAMB Pytorch code, on the other hand, verified and referenced from Pytorch Optimizer<sup>3</sup>. Besides, the warm-up strategy Gotmare et al. (2019) contains two separate stages: linear learning rate scaling and learning rate decay. In this first stage,  $\gamma_t$  becomes greater gradually by iteratively updating  $\gamma_t = \gamma_{\text{target}} \times \frac{t}{T}$  for each step ( $T = 20$  epochs). Then,  $\gamma_t$  goes down moderately by  $\gamma_t = \gamma_{\text{target}} \times q + \gamma_{\text{min}} \times (1 - q)$  where  $q = \frac{1}{2} \times (1 + \cos \frac{\pi t}{T})$ , which is also conducted in Zbontar et al. (2021); Chen et al. (2020); Bardes et al. (2022). In experiments where LARS and LAMB are conducted without a warm-up strategy, a simple Polynomial Decay is applied instead. TVLARS, on the contrary, is conducted without using a learning rate scheduler.

**Hyperparameters and System.** The learning rates are determined using the square root scaling rule Krizhevsky (2014), which is described detailedly at 5.2.2 (see more results at G). We consider the following sets of  $\gamma_{\text{target}}$ :  $\{1, 2, 3\}$ ,  $\{2, 3, 4\}$ ,  $\{5, 6, 7\}$ ,  $\{8, 9, 10\}$ ,  $\{10, 12, 15\}$ , and  $\{15, 17, 19\}$ , which are associated with  $\mathcal{B}$  of 512, 1024, 2048, 4096, 8192, and 16384, respectively. Otherwise,  $w_d$ , and  $\mu$  is set to  $5 \times 10^{-4}$ , and 0.9, respectively. Besides, all experiments are conducted on Ubuntu 18.04 by using Pytorch Paszke et al. (2019) with multi Geforce 3080 GPUs settings, along with Syncing Batch Normalization, which is proven to boost the training performance Krizhevsky (2014), Yao et al. (2021), Huang et al. (2018).

## B PROOF ON THEOREM 1

Revisit the Definition 1, we have:

$$g_i^t = \bar{g}^t + \Delta g_i^t. \quad (6)$$

In applying the large batch gradient descent with batch size  $\mathcal{B}$ , we have:

$$g_{\mathcal{B}}^t = \frac{1}{\mathcal{B}} \sum_{i=1}^{\mathcal{B}} g_i^t = \frac{1}{\mathcal{B}} \sum_{i=1}^{\mathcal{B}} \bar{g}^t + \Delta g_i^t = \bar{g}^t + \frac{1}{\mathcal{B}} \sum_{i=1}^{\mathcal{B}} \Delta g_i^t. \quad (7)$$

Apply the  $L^2$  Weak Law (Durrett, 2010, Theorem 2.2.3), we have:  $g_{\mathcal{B}}^t \leq \bar{g}^t + \frac{\sigma^2}{\mathcal{B}}$ , which can be also understood as:

$$\mathbb{E}_{x_i, y_i \in \{\mathcal{X}, \mathcal{Y}\}} [\bar{g}^t - g_{\mathcal{B}}^t] \leq \sigma^2 / \mathcal{B} \quad (8)$$

<sup>1</sup><https://github.com/facebookresearch/barlowtwins>

<sup>2</sup><https://github.com/Lightning-Universe/lightning-flash>

<sup>3</sup><https://github.com/jettify/pytorch-optimizer>

## C TIME VARYING COMPONENT BOUND

Consider the following equation of time-varying component:

$$\phi(t) = \frac{1}{\alpha + \exp\{\lambda(t - d_e)\}} + \gamma_{\min} \quad (9)$$

We then analyze its derivative (Equation 10) to gain deeper insights into how it can affect the gradient scaling ratio.

$$\frac{\partial\phi(t)}{\partial t} = \frac{-\lambda \exp\{\lambda t - \lambda d_e\}}{(\alpha + \exp\{\lambda t - \lambda d_e\})^2} \leq 0 \quad \text{w.r.t.} \quad \begin{cases} (\alpha + \exp\{\lambda t - \lambda d_e\})^2 \geq 0 \\ \lambda \exp\{\lambda t - \lambda d_e\} \geq 0 \end{cases} \quad (10)$$

Thus function  $\phi(t)$  is a decreasing function for any  $t \in [0, T)$ . Therefore the minimum value of the above function at  $T \rightarrow \infty$  is  $\gamma_{\min}$  (Equation 11).

$$\min\{\phi(t)\} = \lim_{t \rightarrow \infty} \frac{1}{\alpha + \exp\{\lambda(t - d_e)\}} + \gamma_{\min} = \gamma_{\min} \quad (11)$$

While the maximum value at the origin point is:

$$\max\{\phi(t)\} = \phi(t = 0) = \frac{1}{\alpha + \exp\{-\lambda d_e\}} \quad (12)$$

Hence the time-varying component has the following bounds:

$$\gamma_{\min} \leq \phi(t) \leq \frac{1}{\alpha + \exp\{-\lambda d_e\}} \quad (13)$$

## D DETAILED ANALYSIS

Overall, it is transparent that TVLARS performs well in most settings followed by LARS and LAMB, especially with batch sizes of 512, 1024, 2048, and 4096 (Table 1). In 512 sampled batch size experiments, TVLARS achieves 78.92, 81.42, and 81.56% on CIFAR10 and 37.56, 39.28, and 39.64% on Tiny ImageNet related to the learning rate of 1, 2, and 3, as opposed to 74.64, 77.49, and 79.64% and 33.72, 36.60, and 38.92% accomplished from LARS, respectively. TVLARS continues to perform better on even higher batch sizes: 1024, 2048, and 4096 with a stable rise in accuracy. While the performance of LARS varies approximately from 75% to 80%, TVLARS gains accuracy nearly or above 82% trained on CIFAR10 with batch sizes of 1024, 2048, and 4096. Furthermore, this assertion remains the same for experiments with Tiny ImageNet that TVLARS stably reaches the accuracy from 38% to 41%, in contrast with mostly from 33% to 38% of LARS. On even higher batch size settings: 8K and 16K, TVLARS achieves more stable performances: from approximately 81% to nearly 83%, and from 36% to above 42% on CIFAR10 and Tiny ImageNet, respectively. Although the performance of TVLARS and LARS are close to each other, the performance of the model trained by LARS accompanied by a warm-up strategy tends to explode and slow convergence in a very high batch size of 16K (see Figure 17c), which attains only 38% on CIFAR10 compared to fast convergence (within 20 epochs) and stable learning of TVLARS (see Figures 29c, 41c, 47c, 53c, 59c), which accomplishes 80.42%. LAMB, on the other hand, plunges to just above poor performance, especially just above 0% experimenting with the two lower learning rates for a batch size of 16K. However, in the highest learning rate considered, LAMB achieves a performance of approximately 80%.

Another interesting point is that the higher the learning rate is, the faster the model reaches the optimal point, which claims that owing to the high learning rate at the initial training phase, the exploration of the loss landscape is enhanced by avoiding the model being trapped by the early poor sharp minima Dinh et al. (2017); Keskar et al. (2017). This phenomenon is indicated evidently in Figures of Section E, especially in experiments with a decay coefficient of 0.0001 used in Table 1. In detail, in the experiment with batch sizes of 512 and 1024, the convergence rate of the objective functions is nearly unchanged, which takes from 20 to 40 (see Figures 42, 43) epochs to reach the optimal point, compared to more than 40 in LARS with warm-up strategy (see Figures 12, 13, 14, 15,

16, 17). Moreover, the objective function value of TVLARS plunges to the optimal value after just above 20 epochs (45, 46, 47), as opposed to nearly 60 and 80 epochs in the experiments of LARS with batch sizes of 4K, 8K, and 16K (15a, 15b, 15c, 16a, 16b, 16c, 17a, 17b, 17c), respectively. This circumstance is caused by the imperfect exploration ability of a small learning rate Li et al. (2019); Keskar et al. (2017) in the warm-up phase, which steadily increases the learning rate from a small learning rate to a target learning rate by iteratively updating the learning rate  $\gamma_t = \gamma_{\text{target}} \times \frac{t}{T}$ . Although LARS and TVLARS ( $B = 16\text{K}$ ) conducted with learning rates of 15 and 17 reach the optimal point after 60 epochs, TVLARS experimented with a learning rate of 19 converges after 20 epochs, in contrast to 20 epochs from LARS. LAMB experiments are not an exception, they tend to reach the optimal point deliberately. Experimented with batch sizes of 4K, 8K, and 16K, for instance, LAMB acquires from 60 to 80 epochs to reach the optimum point for all learning rates considered (9, 10, 11).

On the other hand, as the ability to avoid the many sharp minima that exist near the weight initialization point by high initial learning rate Hoffer et al. (2017), Kim et al. (2021), TVLARS enhances the model by finding a better performance local minima (see Figures 42a, 42b, 42c, 43a, 43b, 43c), which dives to 0.6 loss value, contrasted to scarcely higher than 1.0 achieved by LARS showed in Figure 12a, 12b, 12c, 13a, 13b, 13c. Especially in larger batch-size training ( $B \in \{8\text{K}, 16\text{K}\}$ ), while TVLARS reach a loss value of under 0.75 (46a, 46b, 46c), LARS reaches to local minima whose performance of approximately 1.0 error (16a, 16b, 16c). Furthermore, TVLARS performance plunges to optimum (error  $\approx 0$ ) (see Figures 47a, 47b, 47c), as opposed to significantly higher than 2 achieved by LARS (17a, 17b, 17c). As a result of the small learning rate, LARS with the warm-up strategy is effortlessly trapped by low-performance sharp minima. This problem is interpreted by the dramatically unpredictable oscillation of  $\|\nabla_w \mathcal{L}(w)\|$  in the early phase, which is shown in Figures 2g, 2h, 2e. Since the norm of model layers' gradient  $\|\nabla w\| = \{\|\nabla w_k\|\}_{k=0}^{K-1}$  varies from 0 to a much larger value frequently after several epochs, the model is stuck by local sharp minima whose different performance Keskar et al. (2017): larger than 20 error value. After 60 to 80 epochs, the model trained by LARS converges without being immobilized by poor sharp minima. This is a result of the ratio  $\|w\|/\|\nabla w\| \rightarrow \infty$  as  $\|\nabla w\| \rightarrow 0$ , which creates a high adaptive learning rate to escape the trapped minima, where  $\|w\|$  gradually decrease after each iteration. The higher the learning rate is, the more expeditious LARS achieves, which converges to a minimum whose loss value of 2 after 80, 70, and 60 epochs with learning rates of 15, 17, and 19, separately. LAMB is not an exception, whose  $\|w\|/\|\nabla w\|$  fluctuate frequently, which indicates the ability of LAMB to tackle the poor performance sharp minima, though its performance is not satisfactory that LAMB's loss value drops to around 1 (6, 7, 8, 9, 10, 11), compared to under 0.5 loss value achieved by TVLARS. However, in the experiments with the largest learning rates considered, LAMB finds it easy to escape the poor sharp minima that the ratio  $\|w\|/\|\nabla w\|$  is not oscillated drastically (see Figures 6c, 7c, 8c, 9c, 10c, 11c), and converge to optimum within 40 epochs whose performance are nearly the same with LARS.

## E FURTHER EXPERIMENTS ON SCALING RATIO

### E.1 LAMB

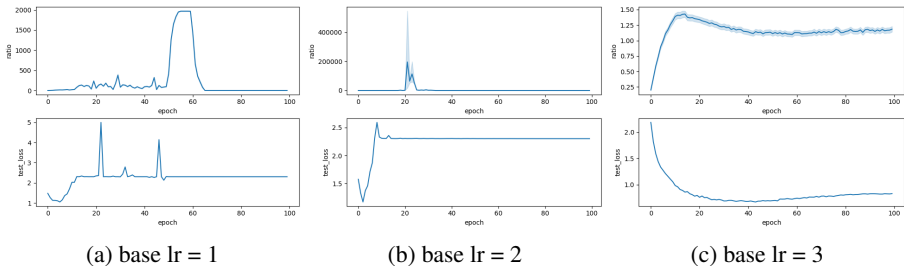


Figure 6: Batch size = 512

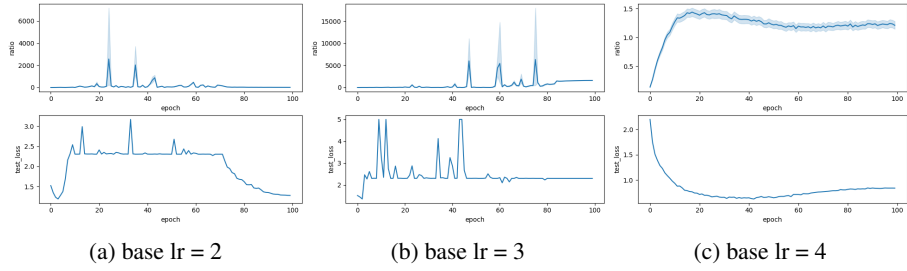


Figure 7: Batch size = 1024

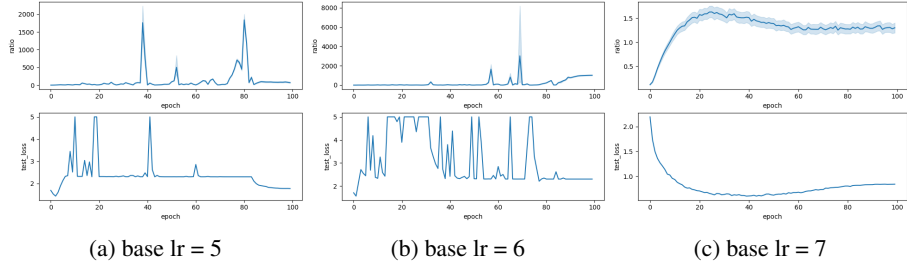


Figure 8: Batch size = 2048

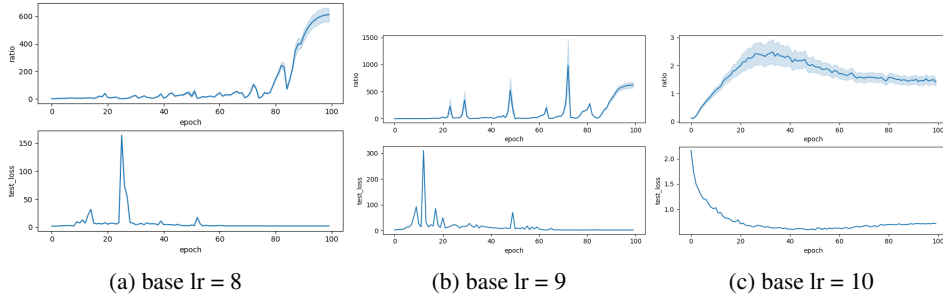


Figure 9: Batch size = 4096

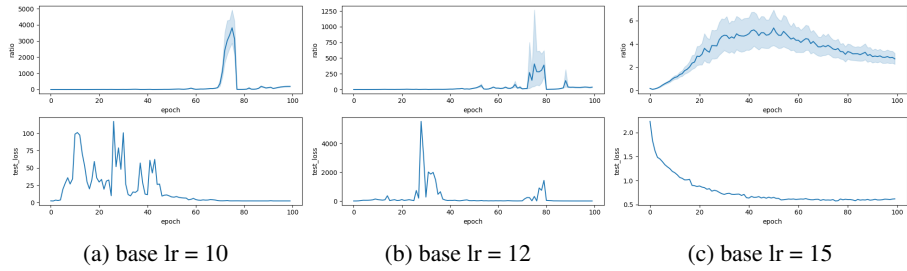


Figure 10: Batch size = 8K

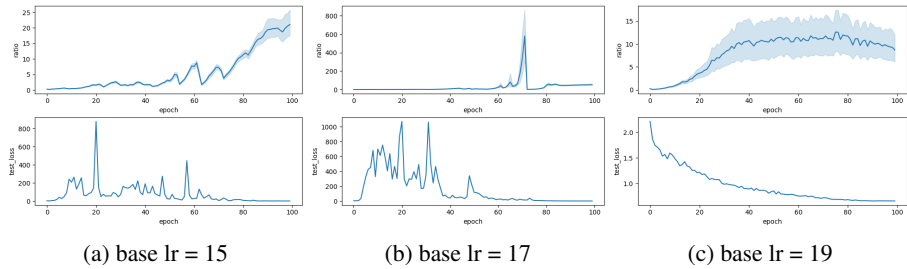


Figure 11: Batch size = 16K

## E.2 LARS

## E.2.1 WITH WARM UP

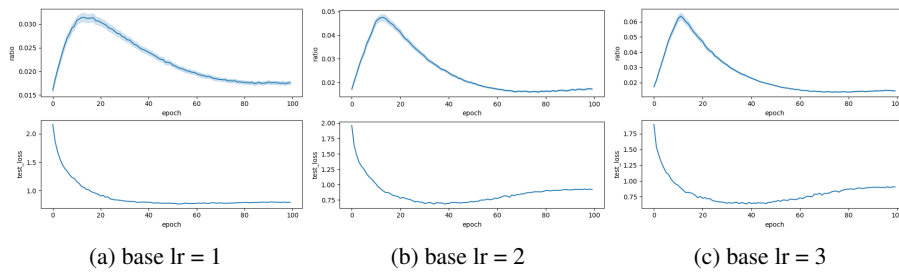


Figure 12: Batch size = 512

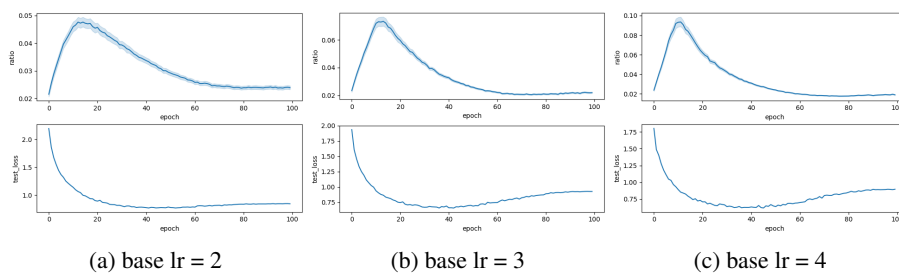


Figure 13: Batch size = 1024

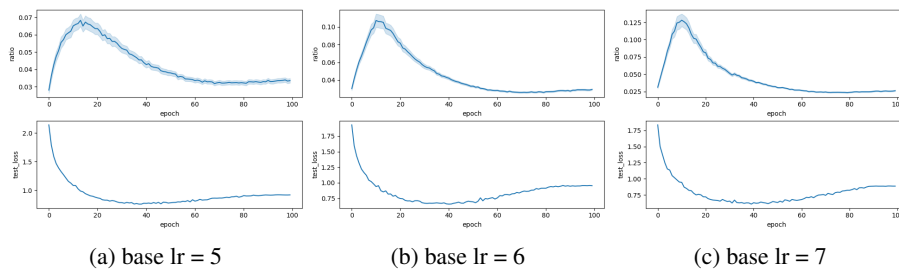


Figure 14: Batch size = 2048

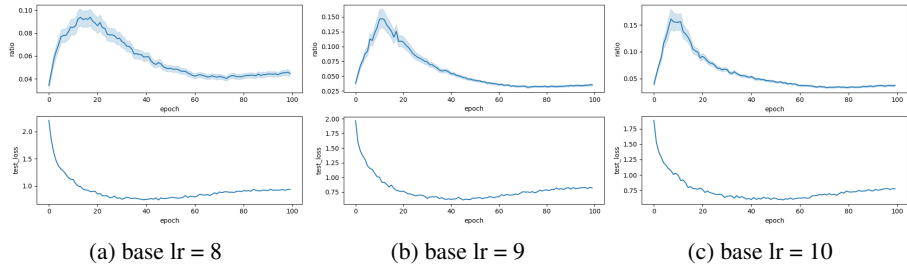


Figure 15: Batch size = 4096

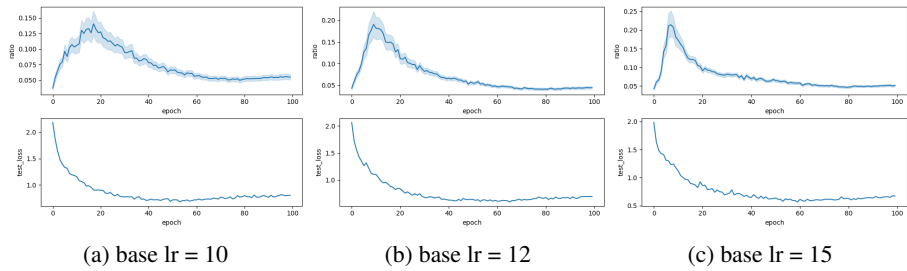


Figure 16: Batch size = 8192

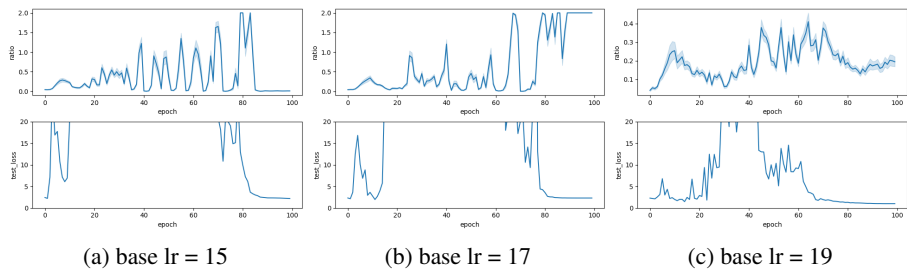


Figure 17: Batch size = 16384

## E.2.2 WITHOUT WARM UP

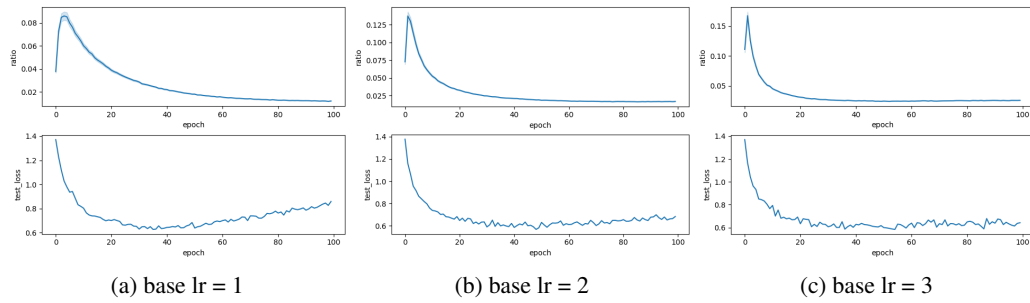


Figure 18: Batch size = 512

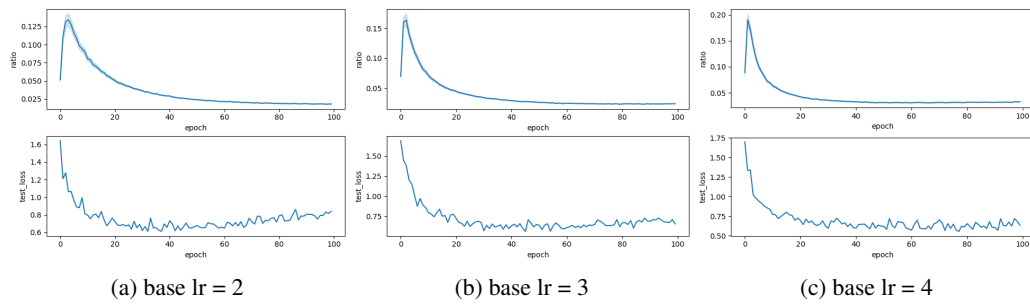


Figure 19: Batch size = 1024

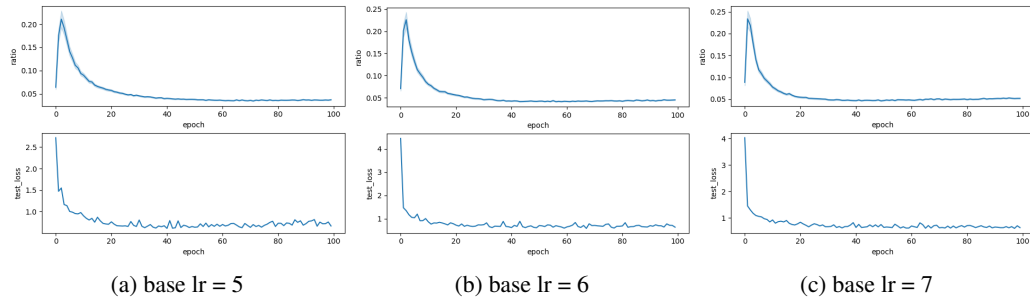


Figure 20: Batch size = 2048

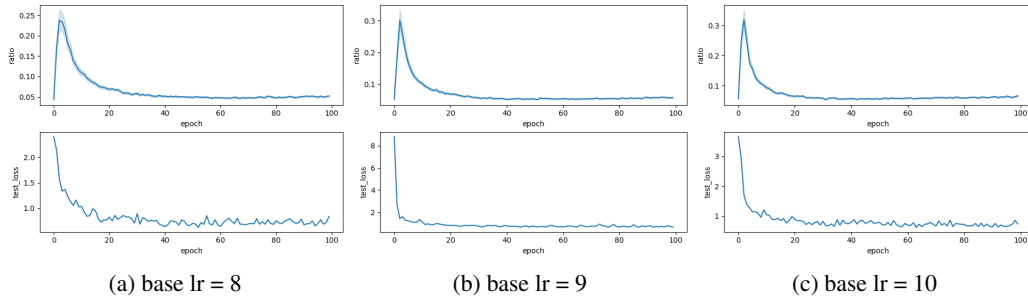


Figure 21: Batch size = 4096

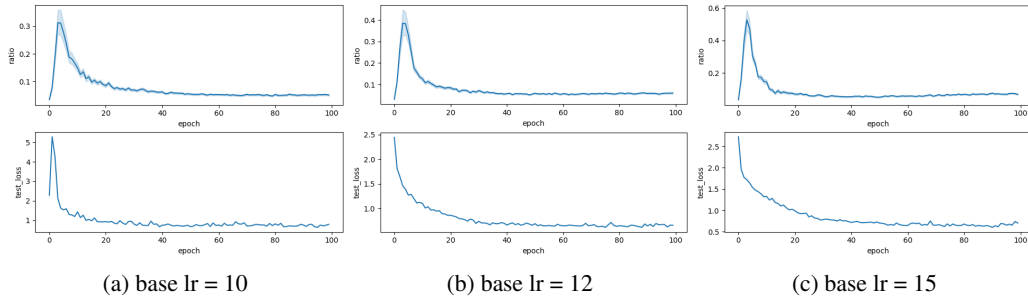


Figure 22: Batch size = 8192

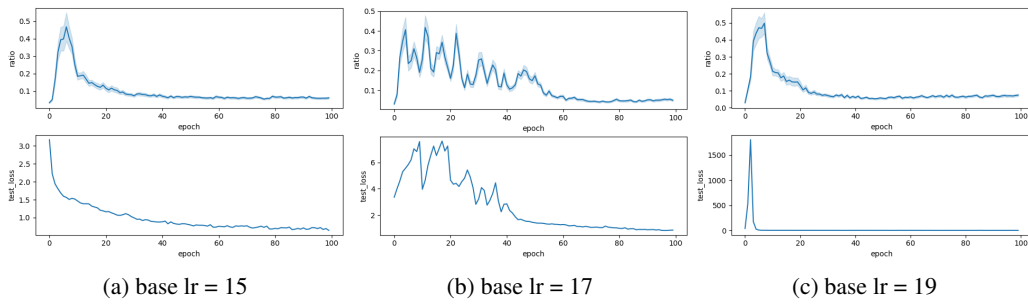
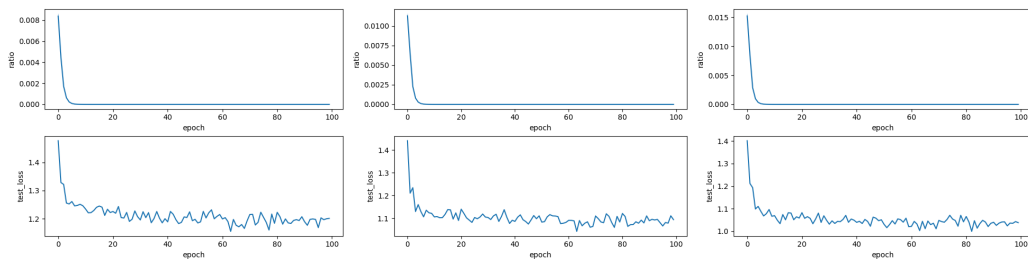


Figure 23: Batch size = 16384

## E.3 TVLARS

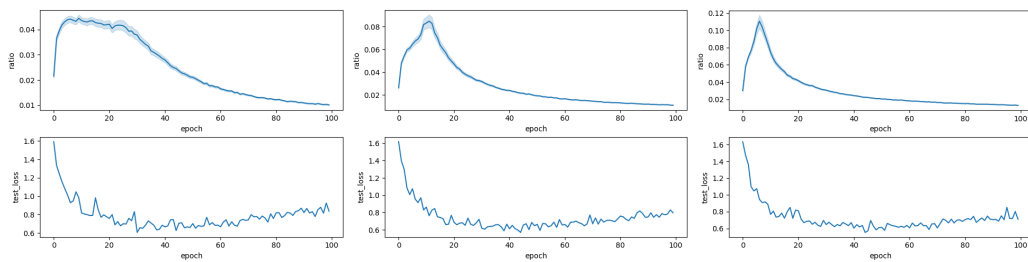
E.3.1  $\lambda = 0.01$ 

(a) base lr = 1

(b) base lr = 2

(c) base lr = 3

Figure 24: Batch size = 512

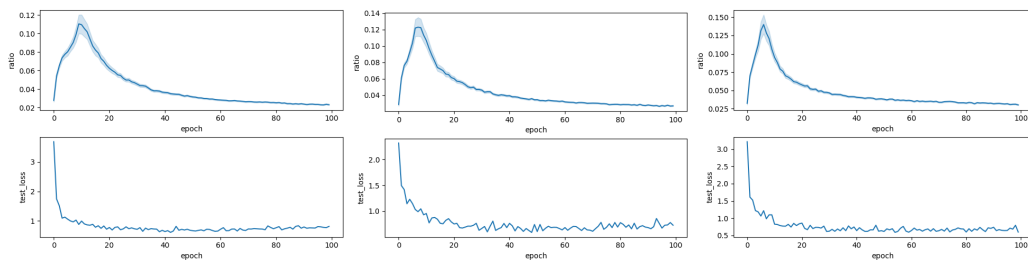


(a) base lr = 2

(b) base lr = 3

(c) base lr = 4

Figure 25: Batch size = 1024



(a) base lr = 5

(b) base lr = 6

(c) base lr = 7

Figure 26: Batch size = 2048

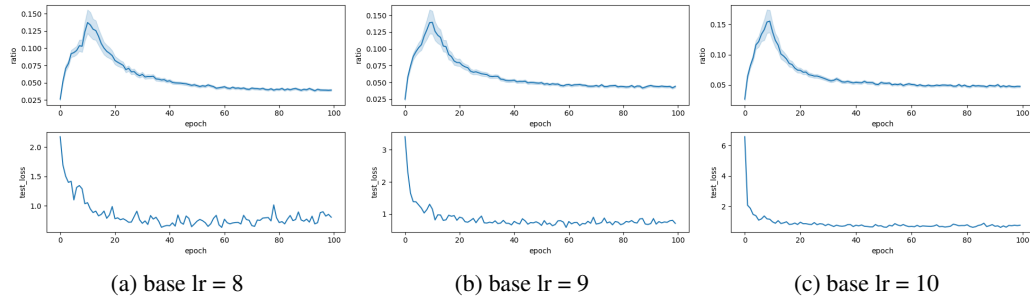


Figure 27: Batch size = 4096

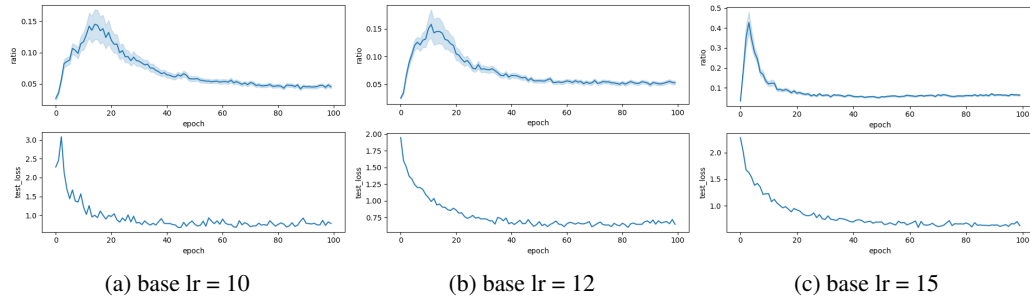


Figure 28: Batch size = 8192

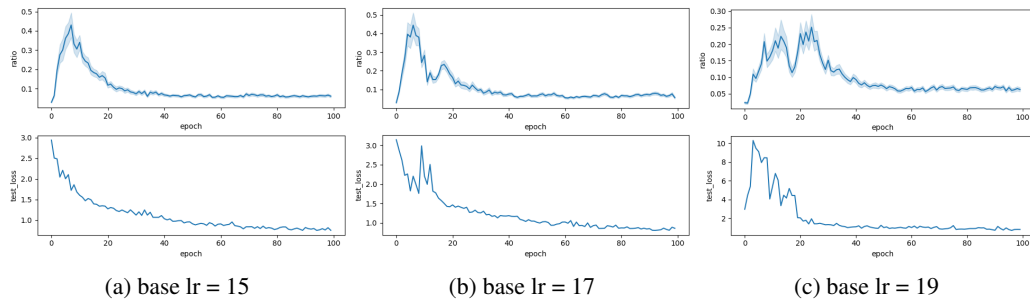


Figure 29: Batch size = 16384

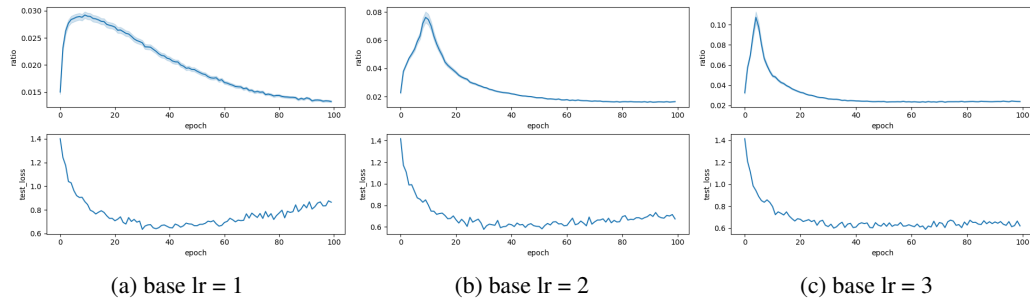
E.3.2  $\lambda = 0.005$ 

Figure 30: Batch size = 512

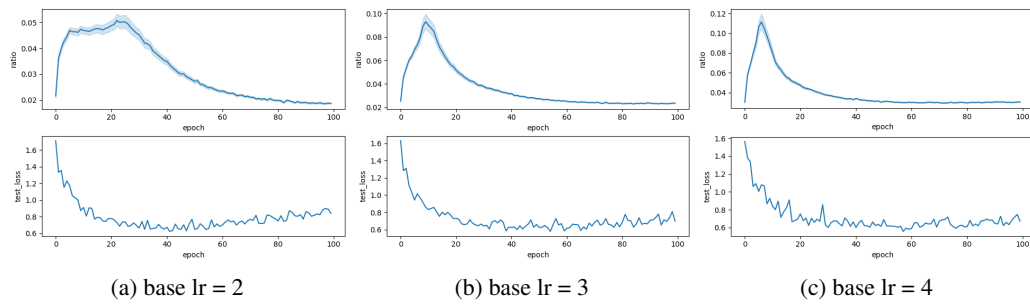


Figure 31: Batch size = 1024

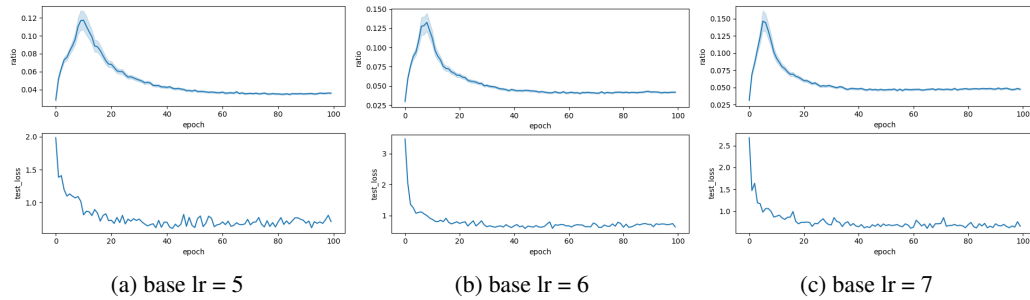


Figure 32: Batch size = 2048

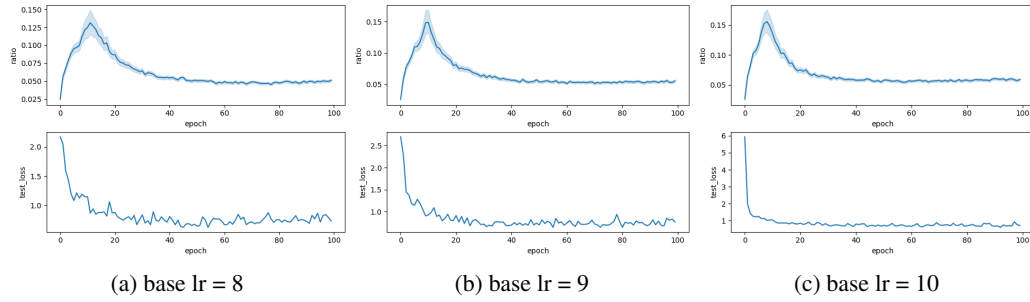


Figure 33: Batch size = 4096

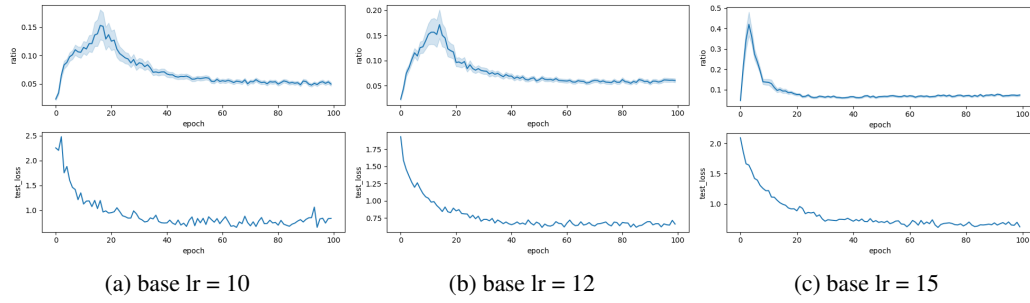


Figure 34: Batch size = 8192

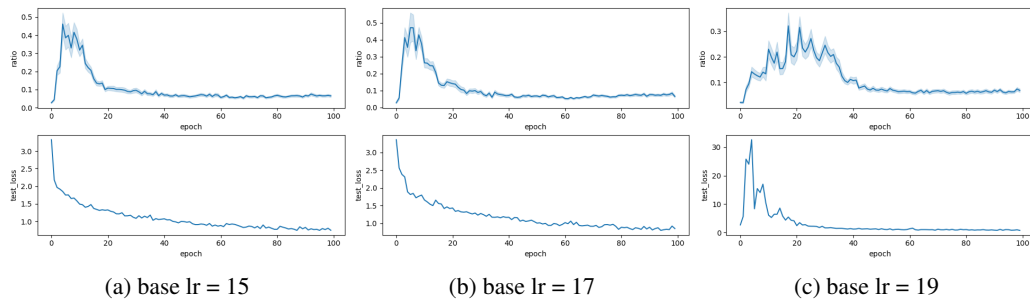


Figure 35: Batch size = 16384

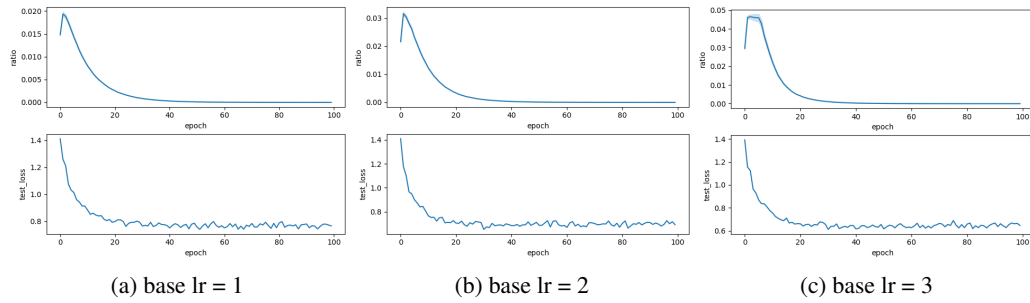
E.3.3  $\lambda = 0.001$ 

Figure 36: Batch size = 512

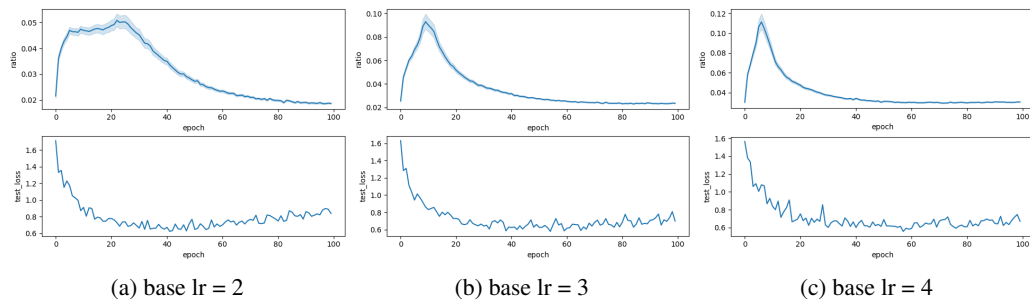


Figure 37: Batch size = 1024

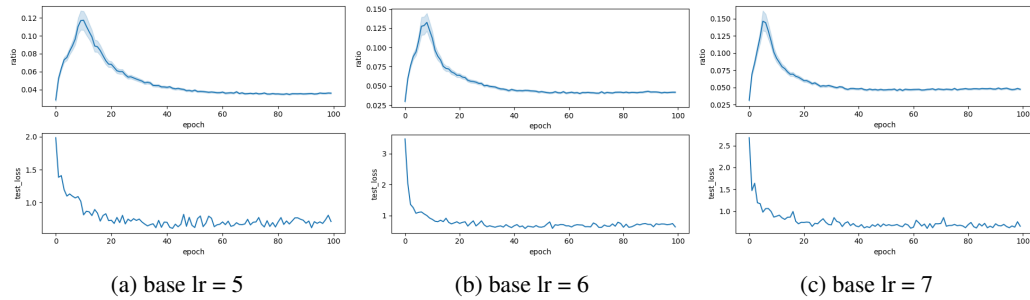


Figure 38: Batch size = 2048

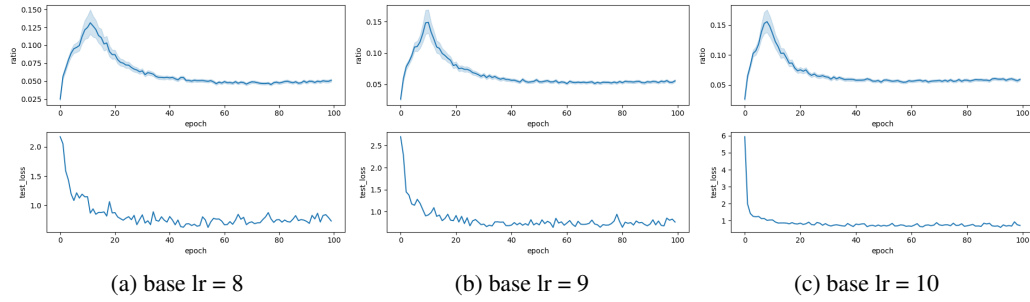


Figure 39: Batch size = 4096

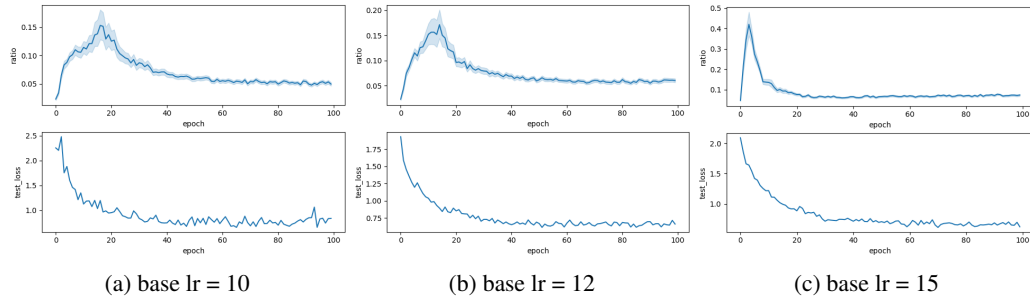


Figure 40: Batch size = 8192

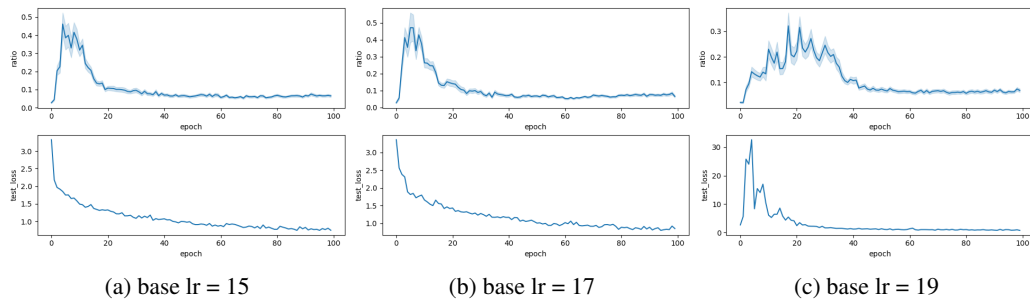


Figure 41: Batch size = 16384

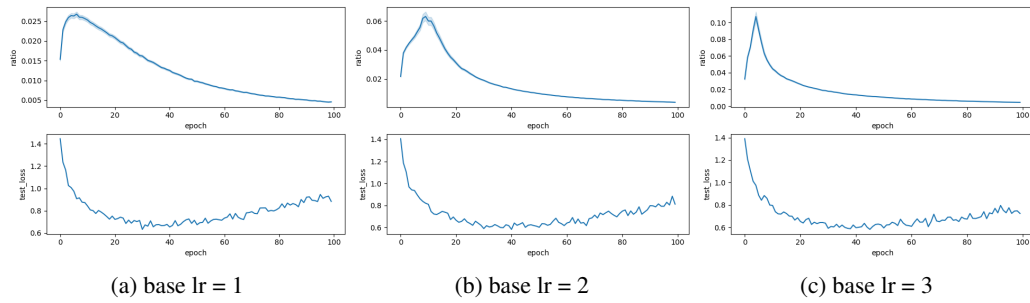
E.3.4  $\lambda = 0.0001$ 

Figure 42: Batch size = 512

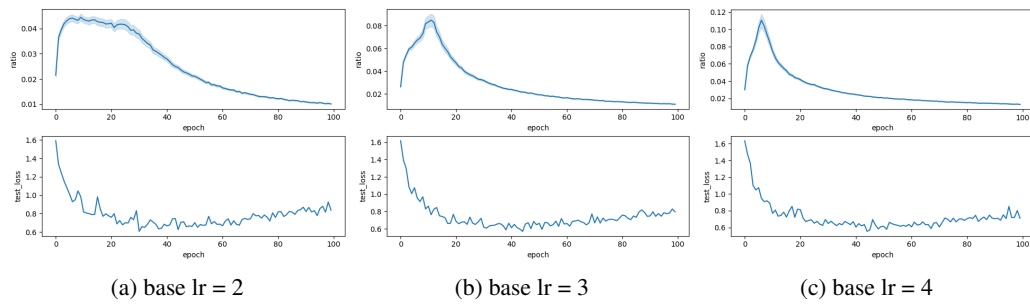


Figure 43: Batch size = 1024

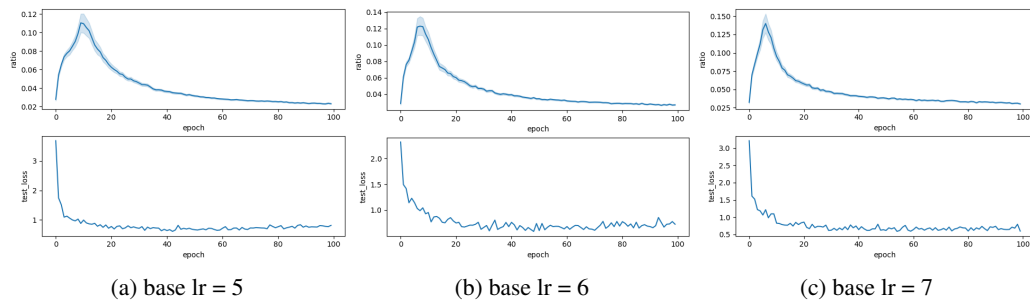


Figure 44: Batch size = 2048

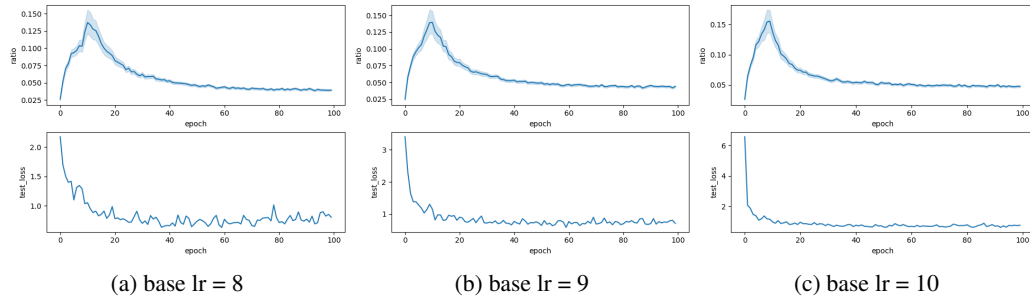


Figure 45: Batch size = 4096

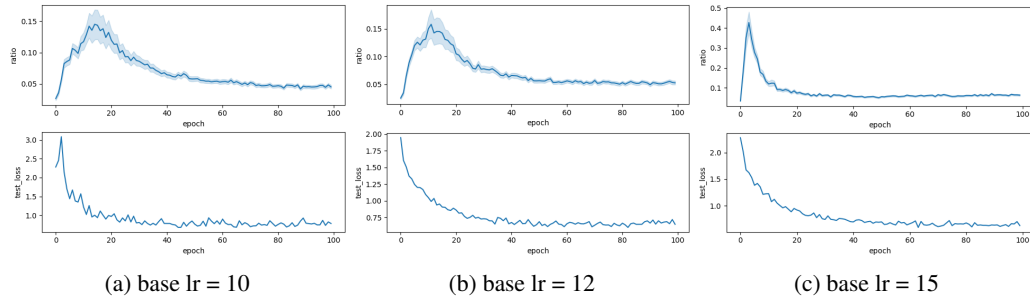


Figure 46: Batch size = 8192

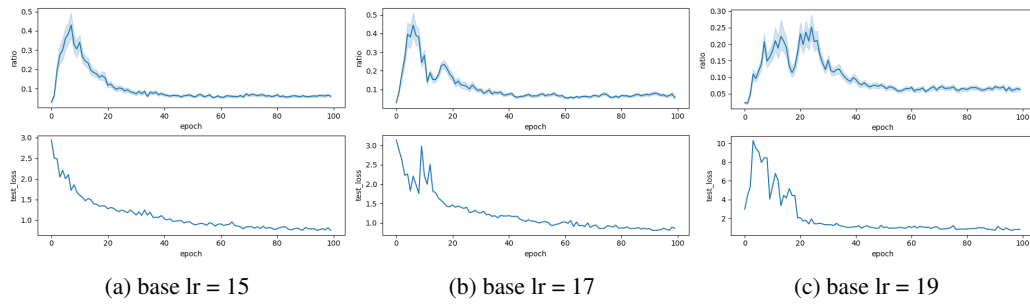


Figure 47: Batch size = 16384

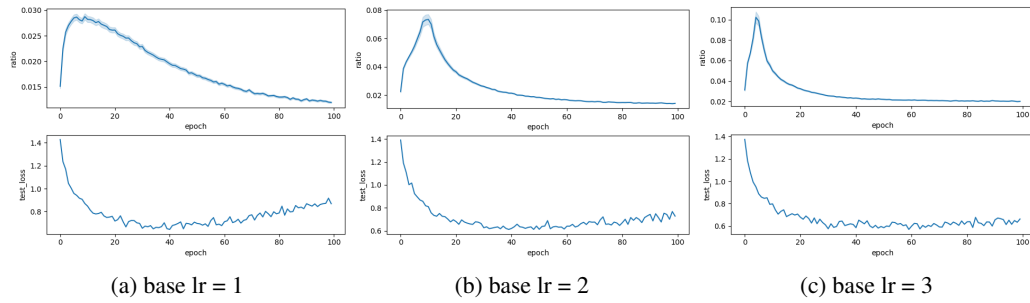
E.3.5  $\lambda = 0.00001$ 

Figure 48: Batch size = 512

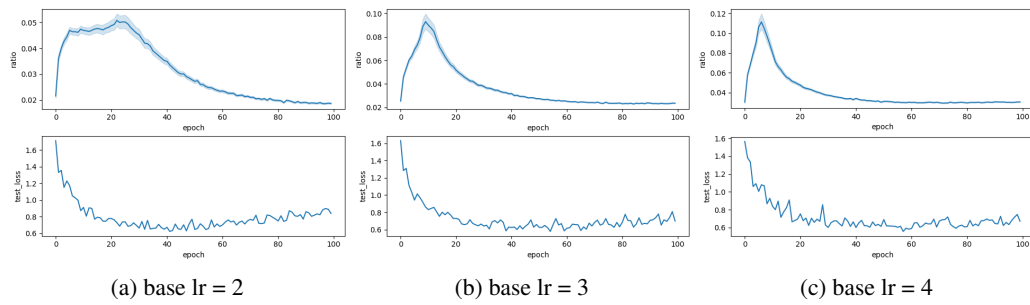


Figure 49: Batch size = 1024

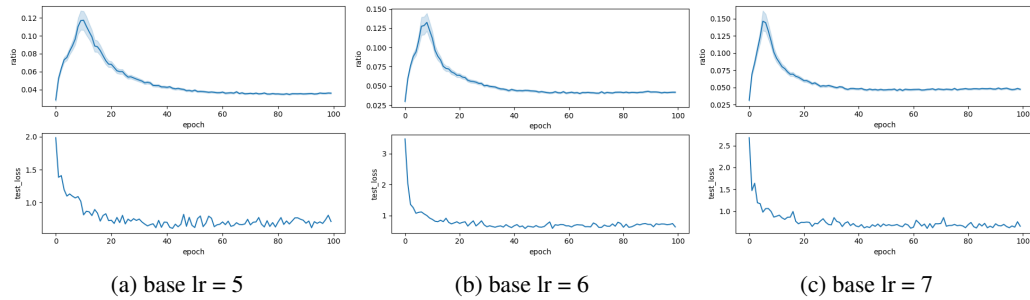


Figure 50: Batch size = 2048

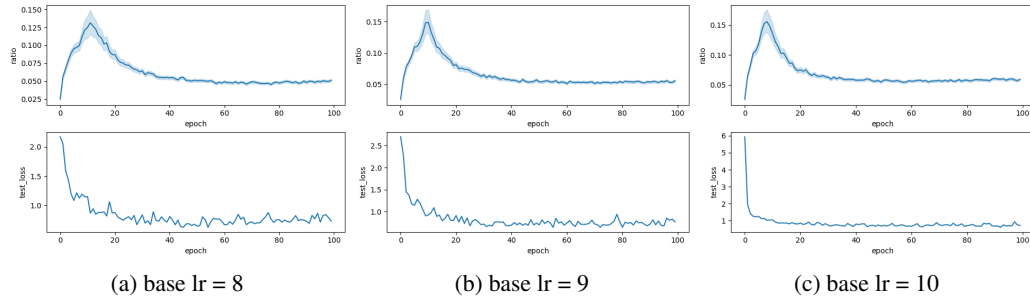


Figure 51: Batch size = 4096

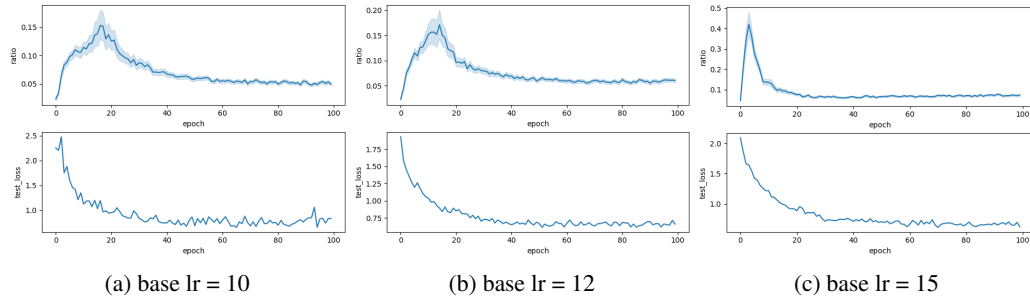


Figure 52: Batch size = 8192

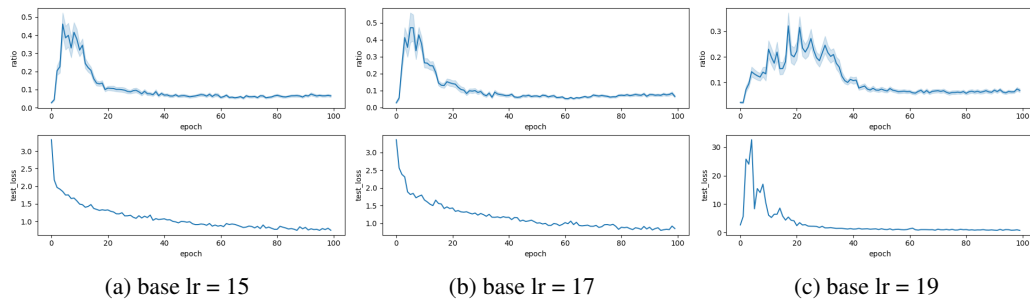


Figure 53: Batch size = 16384

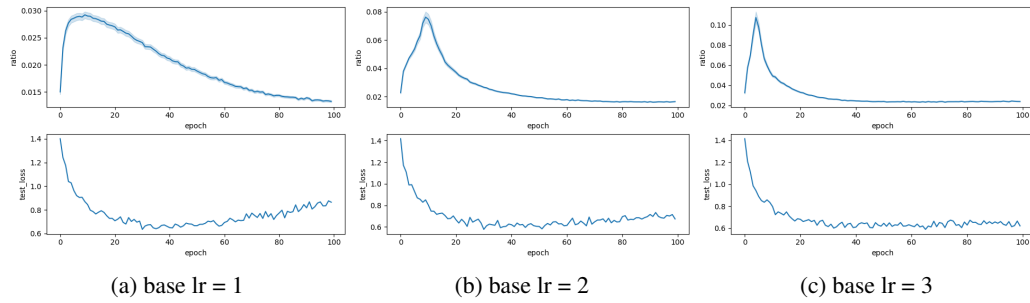
E.3.6  $\lambda = 0.000001$ 

Figure 54: Batch size = 512

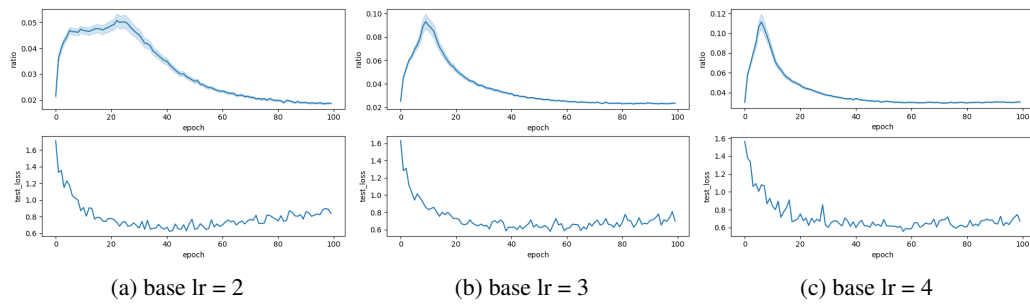


Figure 55: Batch size = 1024

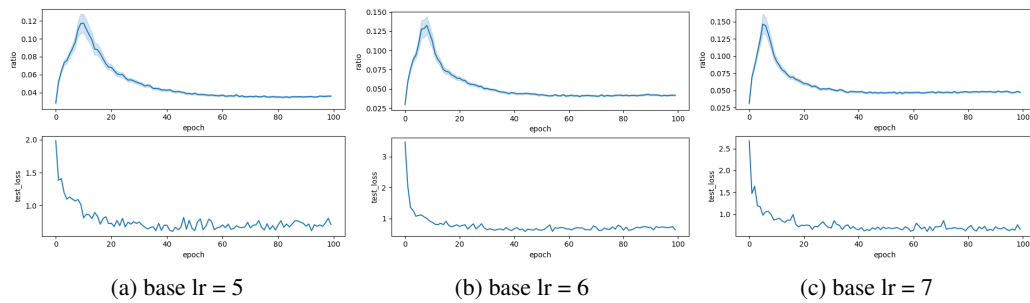


Figure 56: Batch size = 2048

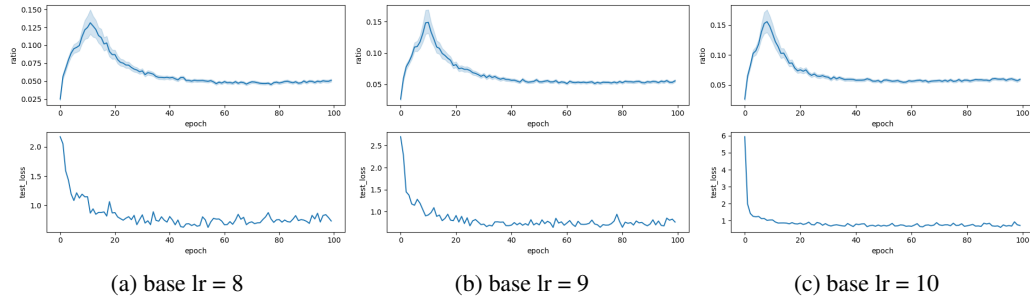


Figure 57: Batch size = 4096

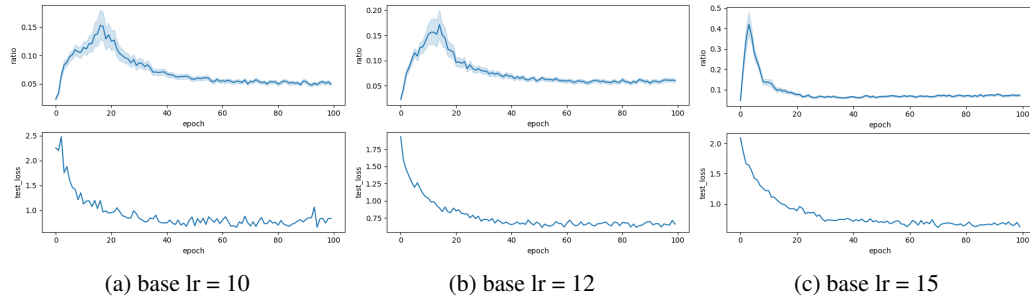


Figure 58: Batch size = 8192

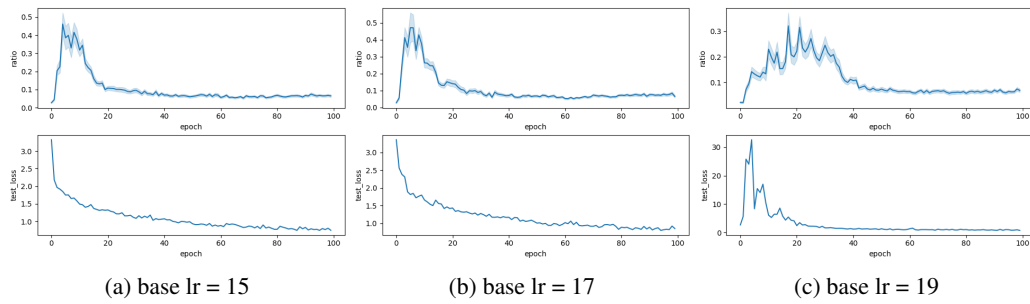


Figure 59: Batch size = 16384

## F FURTHER EXPERIMENT ON LARS WITH AND WITHOUT WARM-UP STRATEGY

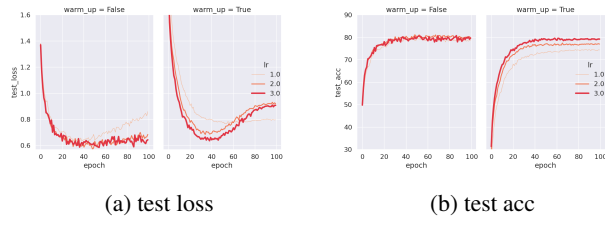


Figure 60:  $\mathcal{B} = 512$

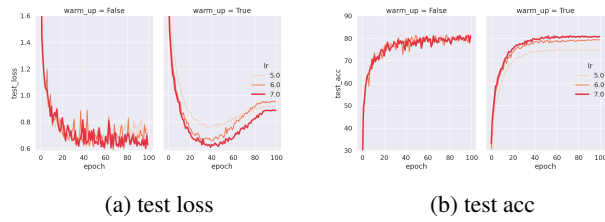


Figure 61:  $\mathcal{B} = 2048$

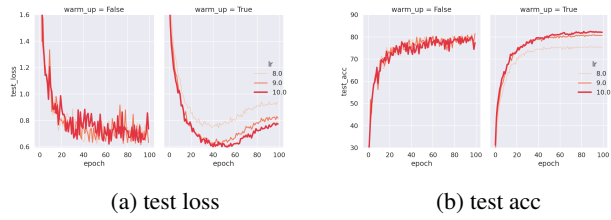


Figure 62:  $\mathcal{B} = 4096$

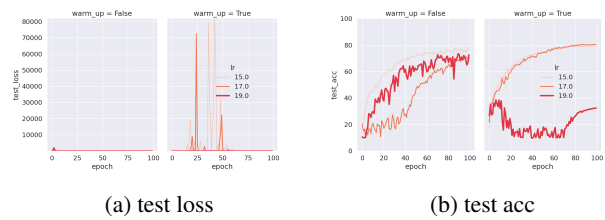
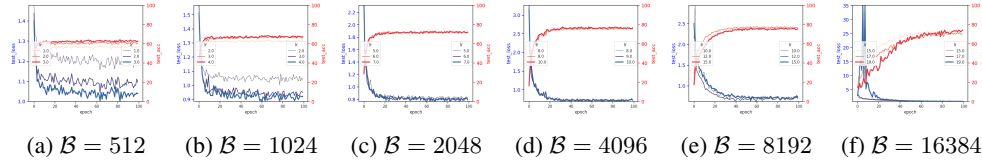
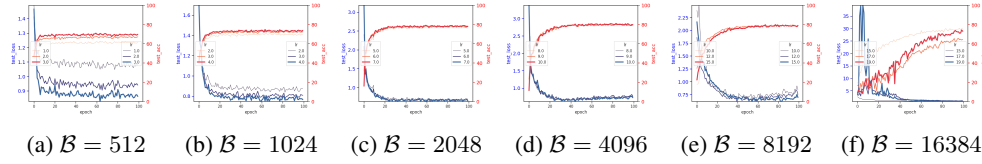
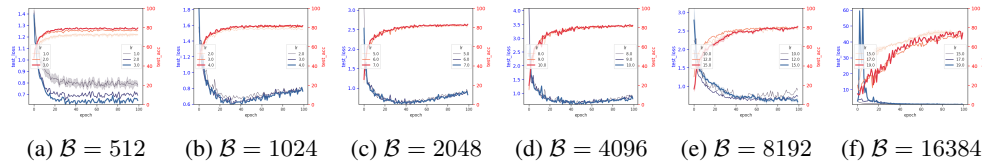
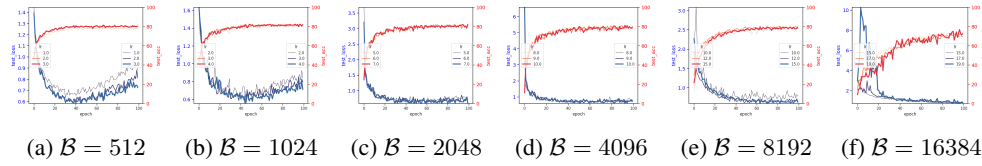
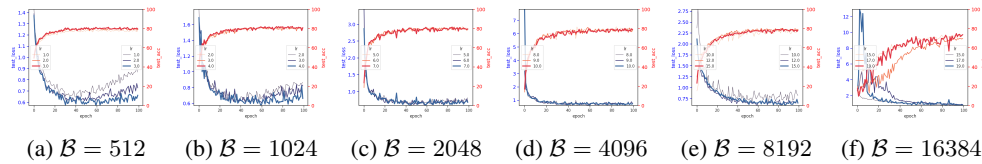
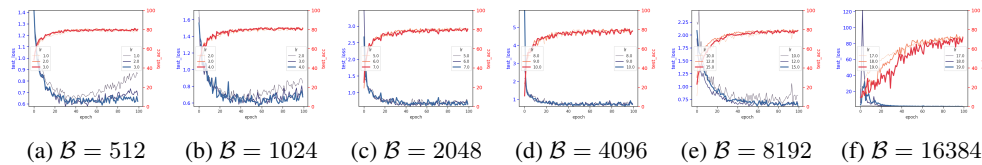


Figure 63:  $\mathcal{B} = 16384$

## G FURTHER EXPERIMENT OF TVLARS WITH A LARGE VARIATION OF DECAY COEFFICIENT

Figure 64:  $\lambda = 0.01$ .Figure 65:  $\lambda = 0.01$ .Figure 66:  $\lambda = 0.001$ .Figure 67:  $\lambda = 0.0001$ .Figure 68:  $\lambda = 0.00001$ .Figure 69:  $\lambda = 0.000001$ .